



Review article

Profiling to Probing: Atomic force microscopy to characterize nano-engineered implants

Karan Gulati^{a,b,*}, Taiji Adachi^a^a Institute for Life and Medical Sciences, Kyoto University, Sakyo, Kyoto 606-8507, Japan^b The University of Queensland, School of Dentistry, Herston QLD 4006, Australia

ARTICLE INFO

Article history:

Received 22 January 2023

Revised 26 July 2023

Accepted 3 August 2023

Available online 9 August 2023

Keywords:

Atomic force microscopy

AFM

Implants

Nanotopography

Characterization

Cell adhesion

Single-cell force spectroscopy

SCFS

ABSTRACT

Surface modification of implants in the nanoscale or implant nano-engineering has been recognized as a strategy for augmenting implant bioactivity and achieving long-term implant success. Characterizing and optimizing implant characteristics is crucial to achieving desirable effects post-implantation. Modified implant enables tailored, guided and accelerated tissue integration; however, our understanding is limited to multicellular (bulk) interactions. Finding the nanoscale forces experienced by a single cell on nano-engineered implants will aid in predicting implants' bioactivity and engineering the next generation of bioactive implants. Atomic force microscope (AFM) is a unique tool that enables surface characterization and understanding of the interactions between implant surface and biological tissues. The characterization of surface topography using AFM to gauge nano-engineered implants' characteristics (topographical, mechanical, chemical, electrical and magnetic) and bioactivity (adhesion of cells) is presented. A special focus of the review is to discuss the use of single-cell force spectroscopy (SCFS) employing AFM to investigate the minute forces involved with the adhesion of a single cell (resident tissue cell or bacterium) to the surface of nano-engineered implants. Finally, the research gaps and future perspectives relating to AFM-characterized current and emerging nano-engineered implants are discussed towards achieving desirable bioactivity performances. This review highlights the use of advanced AFM-based characterization of nano-engineered implant surfaces via *profiling* (investigating implant topography) or *probing* (using a single cell as a probe to study precise adhesive forces with the implant surface).

Statement of significance

Nano-engineering is emerging as a surface modification platform for implants to augment their bioactivity and achieve favourable treatment outcomes. In this extensive review, we closely examine the use of Atomic Force Microscopy (AFM) to characterize the properties of nano-engineered implant surfaces (topography, mechanical, chemical, electrical and magnetic). Next, we discuss Single-Cell Force Spectroscopy (SCFS) via AFM towards precise force quantification encompassing a single cell's interaction with the implant surface. This interdisciplinary review will appeal to researchers from the broader scientific community interested in implants and cell adhesion to implants and provide an improved understanding of the surface characterization of nano-engineered implants.

© 2023 The Author(s). Published by Elsevier Ltd on behalf of Acta Materialia Inc.

This is an open access article under the CC BY-NC-ND license

<http://creativecommons.org/licenses/by-nc-nd/4.0/>

1. Introduction

Implants are routinely placed to correct or replace tissues like bones or teeth, and surface modification of implants in the micro-

and nanoscales has been performed to augment bioactivity [1,2]. Various investigations have confirmed that nano-engineered implants outperform micro-scale modifications in achieving timely establishment and long-term maintenance of implant integration [3]. Multiple strategies, including physical (sputtering, plasma, laser, physical vapour deposition), chemical (acid-etching), electrochemical (anodization), and biological (hydroxyapatite, Ca/P) treatments have enabled the nano-engineering of implants [4]. Implant nano-engineering has shown favourable outcomes in augmenting

* Corresponding author at: The University of Queensland, School of Dentistry, Herston QLD 4006, Australia.

E-mail address: k.gulati@uq.edu.au (K. Gulati).

bioactivity (implant-tissue integration) and achieving local therapy [5].

Soon after implantation, the implant surface encounters a foreign body reaction via a complex interplay of protein adsorption and resident cell infiltration [6]. The initial protein adhesion can dictate subsequent implant-tissue integration. Implant surface characteristics, including topography and chemistry, modulate biochemical signals that control cell-matrix interaction [7]. A fundamental aspect of cell functioning is adhesion which involves integrin receptor-ligand binding/clustering to form focal adhesion complexes [8,9]. Further, the emerging nanoscale-modified implants allow for the manipulation of ligands for cell adhesion receptors enabling control of focal adhesion on cells and, thus, cellular functions [7].

For orthopaedic and dental implants, integration between the implant and surrounding tissue is crucial to implant success and continuing battle against bacterial ingress [10,11]. *Race to invade* phenomenon often dictates the success of implants, with numerous cells *racing* to adhere and attach to the implant surface, including the ever-present bacteria (applicable to dental implants) [12]. Since cellular biomechanics operate at the nanoscale [13], nano-engineered implants have been used to augment cell adhesion and functions [14]. Considering that cells respond to the surrounding mechanical cues via actin-based structures lamellipodia and filopodia, to better understand cell biomechanics and the relationship between such structures and the nanoscale modified surface, precise measurement of the dynamic forces from the single-molecule to the entire cell level is needed.

Atomic force microscopy (AFM) is a unique and precise nanomechanical characterization tool that allows the manipulation of a single molecule or single cell to record minute forces of interactions when the molecule/cell interacts with a substrate [15,16]. The cellular ability to remain attached under detachment force application is the basis for quantifying cellular adhesion strength or single-cell force spectroscopy (SCFS). Forces of interaction between a cell and the substrate surface are in nano-newtons (nN), and molecule-substrate are in pico-newtons (pN), and quantifying these interactions onto a nano-engineered implant requires the ability to manipulate a single molecule/cell with high precision and record interacting forces with high-resolution [17,18]. Varied SCFS assays and their pros/cons are reviewed by Friedrichs et al. and Ungai-Salánki et al. [17,19]. Several strategies enable the quantification of adhesion forces and binding kinetics, in physiologically relevant conditions, at both single-cell and single-molecule levels. Among the different SCFS assays, including plate-and-wash, flow chamber, step-pressure, centrifugation, and optical tweezers, commercially available and widely utilized AFM stands out, attributed to control over contact (cell-substrate) conditions, high force resolution and wide range of applicable forces [20]. Briefly, AFM-SCFS is the most versatile SCFS technique, as it enables the investigation of cellular interactions with other cells, proteins and substrates and the detection of forces (10 pN to 100 nN) with precise control [spatial (1 nm–100 μ m) and temporal 0.1 s - > 10 m)] [17,21].

Cellular functions such as migration, proliferation and differentiation depend on the cellular ability to sense and respond to the surface topography and chemistry of the environment/implant [22,23]. Hence, cell adhesion and response are vital characteristics that must be well understood to develop highly bioactive surfaces. The ability to characterize implant surface topography/roughness and single-cell/molecule mechanobiology make AFM a powerful tool for quantifying these functions in physiologically relevant conditions [24,25]. Especially recruitment of a single molecule/cell as a probe to reveal the unique adhesion force signature to specific surface features via SMFS/SCFS holds significant potential in evaluating and predicting implant bioactivity. This extensive review discusses the use of AFM to characterize nanoscale topography (*pro-*

fling); and single-cell interactions (*probing*) that would enable an improved understanding of the implant bioactivity (Fig. 1).

2. Atomic force microscopy

2.1. Working principle

The AFM operation is based on the interaction between a sharp probe tip and a sample surface and involves the following main steps [26,27]:

- **Probe and Cantilever.** AFM uses a cantilever with a sharp tip attached at its end, and the cantilever acts like a flexible spring that deflects in response to the forces exerted between the tip and the sample surface.
- **Approach.** As the AFM probe is brought close to the sample surface and the tip approaches the surface, the interaction forces (electrostatic, van der Waals or chemical bonds) between the tip and the atoms/molecules on the surface come into play.
- **Deflection.** The deflection of the cantilever is measured, typically by reflecting a laser beam off the back of the cantilever onto a photodetector. As the cantilever deflects due to the interaction forces, the position of the laser spot on the detector changes, allowing for deflection measurement.
- **Feedback.** A feedback control loop maintains a constant deflection or force between the tip and the sample surface. The control system adjusts the z-axis position to keep the deflection or force constant, which results in a topographic map of the sample surface.
- **Scanning.** The AFM probe is scanned across the sample surface in a raster pattern, typically using piezoelectric scanners. At each point, the deflection or force is measured and recorded, allowing for the generation of a 2D/3D image of the surface topography.
- **Analysis.** The acquired data is processed/analyzed to generate the final image. By converting the deflection/force measurements into height information, a high-resolution topographic map of the sample surface can be reconstructed.

2.2. Operation modes

Depending on the specific experimental requirements, AFM can also be operated in various modes, including contact, tapping, non-contact, or dynamic modes [28]. These modes involve different interactions and measurement techniques, as described below:

- **Contact.** In contact mode, the AFM probe tip continuously makes physical contact with the sample surface. As a result, the cantilever is deflected due to the interaction forces between the tip and the surface. This mode provides high-resolution topographic images but can be susceptible to tip-sample damage or wear.
- **Tapping.** Tapping mode (intermittent contact mode or dynamic mode) involves oscillating the cantilever at/near its resonance frequency, with the tip lightly tapping or intermittently touching the sample surface during the scanning. This mode reduces tip-sample interaction forces and is useful for imaging soft/delicate samples.
- **Non-Contact.** Non-contact mode operates with the tip oscillating very close to (but not in contact with) the sample surface. The cantilever motion is influenced by the long-range forces (such as van der Waals) between the tip and the surface. This mode is suitable for imaging delicate or easily damaged samples and provides high-resolution topographic information.
- **Force Spectroscopy.** It involves measuring the forces between the tip and the sample as a function of distance or time, and

Nano-Engineered Implants & Their Surface Bioactivity Characterization via AFM

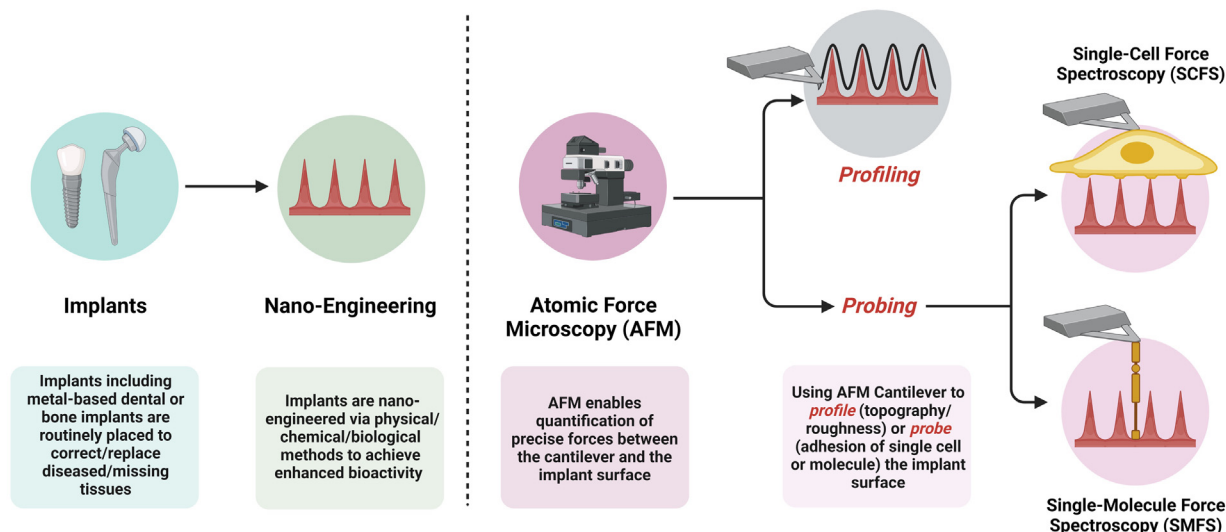


Fig. 1. Profiling to Probing. Schematic representation showing the use of atomic force microscopy (AFM) towards characterizing the bioactivity of nano-engineered implant surfaces. *Profiling via AFM*: quantifying surface topography/roughness and *probing via AFM*: use of a single cell/molecule to probe implant surface to quantify adhesion.

quantifies mechanical properties (adhesion, stiffness, elasticity or friction) at the nanoscale.

- **Scanning Kelvin Probe Force Microscopy (SKPFM).** It combines AFM with electrical measurements and measures the local contact potential difference (CPD) between the probe tip and the sample surface during scanning, enabling the mapping of surface potential variations, electrical conductivity and work function measurements.
- **Magnetic Force Microscopy (MFM).** MFM utilizes a magnetic-coated tip to measure magnetic interactions between the tip and the sample surface and allows for visualizing magnetic domains, magnetic field gradients and magnetic properties of materials.

2.3. Advantages of AFM

AFM permits manipulation at the nanoscale that has significantly influenced developments across various fields [29]. AFM can be used as:

- Microscope with atomic resolution
- Manipulating complex molecules
- Local delivery of molecules
- Nanofabrication tool
- Cell biology (mechanics, division, metabolism and deformation)
- Diagnostics

AFM offers several advantages:

- **Atomic Resolution.** AFM provides exceptional spatial resolution, allowing for imaging and measurement at the nanoscale that can reveal fine surface details and structures with sub-nanometer or atomic-level precision [30]. Hence, AFM can be used to investigate surface topography, roughness, and material properties.
- **Substrate Flexibility.** AFM can be used to image a variety of substrates, including hard materials (metals, ceramics), soft materials (polymers, biomolecules), and biological specimens (cells, tissues). Further, it can operate in various environments, such as air, liquid, or controlled atmospheres, adapting to different experimental requirements.
- **3D Surface Profiling.** AFM enables 3D mapping of the substrate surface, revealing detailed topographic information that is valu-

able for characterizing surface roughness, measuring film thickness, or analyzing surface features/defects.

- **Versatile Modes for Imaging.** AFM offers multiple imaging modes (contact, tapping, non-contact, and dynamic modes) that provide complementary substrate information, including surface imaging, material characterization, mechanical mapping, and chemical analysis.
- **Force Measurements (Mechanical Mapping).** AFM can measure mechanical properties at the nanoscale, such as elasticity, stiffness, and adhesion. This enables the quantification of material properties, cell mechanics analysis, and intermolecular forces investigation.
- **Real-Time Imaging/Manipulation.** AFM provides real-time imaging to observe dynamic processes and interactions at the nanoscale. Further, advanced AFM techniques enable substrate nano-engineering via force application, nanolithography and manipulation of nanoparticles/biomolecules.
- **Easy Substrate Preparation.** Being a non-destructive technique, AFM does not require staining or labelling of the substrates to be analyzed. Additionally, AFM can operate in ambient conditions without extensive substrate preparation, preserving their functionality.

2.4. Limitations of AFM

AFM has several limitations that must be optimized as per the specific requirements of experiments:

- **Slow Scanning Speed.** AFM is a slow imaging technique, especially when imaging large areas or multiple samples. This limitation can hinder high-throughput experiments or time-sensitive studies.
- **Complex Instrumentation.** AFM instruments are complex and require expertise to operate effectively. The instrument setup, calibration, probe preparation, and handling can be technically demanding. As a result, proper training and experience are essential to obtain accurate and reliable results.
- **Probe Cost.** AFM probes have a limited lifetime and can degrade over time or during imaging/analysis, and the cost of high-quality probes can be relatively high, and can add to the overall experimental expenses.

- **Environmental Sensitivity.** AFM measurements can be sensitive to environmental conditions (temperature, humidity, etc.) that can affect the instrument stability and hence the acquired data.
- **Sample Artifacts.** The interaction between the AFM probe and the substrate may cause deformation, scratching, or indentation, particularly for soft or delicate substrates.
- **Limited Imaging in Liquid.** AFM imaging in liquid environments can be difficult attributed to the increased forces and hydrodynamic effects. The presence of liquid can affect the cantilever stability and introduce noise in the images/graphs. Specialized AFM techniques, such as liquid cell AFM can be used to overcome these challenges. *Liquid cell AFM* allows for imaging and manipulation of samples in liquid environments, whereby the substrate of interest is placed within a liquid-filled chamber that is compatible with AFM measurements. The liquid cell provides a controlled/stable environment that allows the substrate to be imaged or manipulated while submerged in a liquid.

2.5. Robotic AFM

Fluid force microscopy (FluidFM) combines AFM with microfluidics to enable force-controlled nanopipetting ability under optical control [29,31]. In FluidFM, the hollow cantilevers inject soluble molecules via a submicrometer aperture in the AFM tip and single living cell stimulation. The dispensing system is force controlled and allows for extreme local liquid injection, and the dispensing tip can be positioned in very close contact with the substrate surface. This allows for precise local dispensing to stimulate cells, pinpoint biomolecules to exact spots, and biochemical analysis [32]. As an alternative to AFM, robotic FluidFM can quantify cell adhesion parameters in a high-throughput manner towards the in-depth evaluation of their population distributions [33,34].

3. Nano-engineering of implant surface

3.1. Basic concepts

- **Implant:** An implant is a medical device or material surgically inserted into the body to replace or support the function of a damaged/missing body part. Examples include dental implants, pacemakers, cochlear implants or joint replacements (hip/knee implants).
- **Implant bioactivity:** It refers to an implant's ability to elicit a specific biological response or interaction with the surrounding biological environment. Bioactive implants promote favourable interactions with the host tissues leading to augmented integration, healing and long-term functionality.
- **Implant Biofouling:** It is the process by which biomaterial/implant surfaces become colonized and contaminated by microorganisms, cells, proteins, or other biological substances. Biofouling can lead to the formation of biofilms, which are complex communities of microorganisms encased in a protective extracellular matrix. These biofilms can cause various complications, including infection, inflammation, reduced functionality of the implant, and ultimately, implant failure.
- **Nano-engineered implant:** A medical implant that has been engineered/modified in the nanoscale (1.0–100 nm) using nanotechnology (for instance, fabricating controlled nanotopography/nanopatterns or using nanomaterials like nanoparticles or nanocomposites) to augment bioactivity, therapy or mechanical characteristics is referred to as a nano-engineered implant. These implants can influence cell behavior, protein adsorption or tissue interactions, enhance cellular adhesion, reduce infections and inflammations, and enable long-term implant success.

3.2. Implant nano-engineering

Various materials, including metals, polymers, or composites, have been used to fabricate prosthetic implants and biomedical devices across orthopedics, dentistry and cardiology [35].

Engineering the surface of implants in the nanoscale (1.0–100 nm) to fabricate controlled implant nanotopographies or nanopatterns (nanopores, nanotubes, nanogrooves, nanopillars or nanopits) on the surface of implants is referred to as 'implant nano-engineering'. Various techniques have been employed to nano-engineer implantable metals, polymers or composites [4,11,36]:

- **Mechanical.** Grinding, machining, blasting and polishing
- **Physical.** physical vapour deposition (PVD), magnetron sputtering, ion implantation, plasma treatment and laser treatment [laser ablation, laser pulse deposition (LPD), matrix-assisted pulsed laser evaporation (MAPLE), direct laser interference patterning (DLIP) [37]
- **Chemical.** Acid or alkaline treatment, sol-gel method, chemical vapour treatment (CVD), supramolecular modifications [layer-by-layer (LBL) assembly]
- **Electrical.** Electrochemical anodization [10,38]
- **Biomolecular.** Proteins, bioactive molecules, peptides or growth factors, calcium phosphate [39,40]

Nano-engineered implants have been used towards tissue regeneration and therapy (local drug delivery) [41,42]. Briefly, nano-engineered implant surfaces can directly influence the biological response, including protein adsorption and cell adhesion/proliferation, to an implant material (via affecting molecular and cellular events) [43]. Utilizing nanotopography to induce desirable cellular responses represents a rapidly growing area in implants [3]. Implant surface topography influences cellular responses at various levels:

- **Macroscale (>100 μm):** affects cells at the colony level
- **Microscale (0.1–100 μm):** influences cells at the single-cell level
- **Nanoscale (1.0–100 nm):** interact with individual cell receptors

3.3. Influence of implant nano-engineering on cellular adhesion and mechanics

Extracellular matrix (ECM) in the cellular micro-environment guides cellular behavior, including integrin ligation and growth factor interaction, that regulate downstream mechanotransductive pathways (cytoskeletal rearrangement and signal cascade activation) [44]. Implant nanotopography strongly influences protein adsorption and modulates ECM conformation, density, and cellular responses. Custom nanotopographies can be used to instruct desirable cellular behaviours, for example, to achieve early establishment and long-term maintenance of implant-tissue integration to ensure implant success [45,46].

Surface topography-induced mechanical signals translate into biochemical signals intracellularly via mechanotransduction [47]. Mechanotransduction is governed by two mechanisms: mechanical signals convert into biochemical signals via biomolecules (indirect mechanotransduction), or mechanical stress/force propagates via the cytoskeleton into the nucleus (direct mechanotransduction) [48]. Cells can sense implant surface topography during adhesion via filopodia (cell membrane projections) equipped with integrins that utilize their 'nanoscale tips' to probe features down to 10nm height [49]. Further, via nanopodia (smaller versions of filopodia), cells can sense sub-10 nm scale surface features [50].

4. AFM-based characterization of nano-engineered implants

AFM is a precise nano-tool that enables the application and sensing of exact minute forces (piconewtons to micronewtons range) on spatially defined areas (sub-nanometres to several tens of micrometres) [51]. Attributed to the characterization of mechanical parameters, including adhesion, force, pressure, elasticity, tension and viscosity, AFM can be utilized to investigate surface topography and single-cell/molecule interactions [52,53], which holds significant potential to test the performance of nano-engineered implants [54].

4.1. Surface topography and roughness

Nanoscale modifications of implants augment protein adhesion and cellular functions or bioactivity. Attributed to mapping surface topography/roughness, ease of operation and low cost, AFM has been widely applied to characterize nanoscale porous thin films [55]. AFM is routinely used to quantify the surface roughness of modified implants, and the roughness corresponds to specific nanotopography or the dimensions of the nanostructures [55]. For instance, AFM imaging provides a 3D spatial overview of nano-engineered implant surfaces to visualize both the micro-roughness and the nanotopography [56]. Further, the average value of root mean square (RMS) and roughness average (Ra) obtained from AFM characterization of implants enables connecting surface topography/roughness to protein and cell adhesion. Implant surface characteristics, including surface area, porosity, topography and roughness, influence protein adhesion capacity, and larger surface areas, nanostructure dimensions and porosity are associated with enhanced protein adhesion [57,58]. Lastly, early adhesion of proteins and cells and accelerated wound healing response post-implantation surgery is promoted on nanoscale rough implants with high surface area [59]. Hence, thorough surface topographical analysis of nano-engineered implants via AFM can help connect topography/roughness with bioactivity.

Several techniques are available to image and quantify nanotopography, allowing for the characterization of surface features and structures at the nanoscale. Some of the commonly used techniques include [27]:

- **Optical Microscopy.** Optical microscopy techniques (employing advanced optical methods, including fluorescence or structured illumination), such as confocal or super-resolution microscopy, can be used to image nanotopography.
- **Interferometry.** White-light interferometry or optical profilometry utilizes the interference patterns created by reflected or scattered light to measure surface topography.
- **X-ray Scattering.** Utilize the scattering patterns of X-rays to analyze the atomic or molecular arrangements. X-ray scattering techniques, such as grazing incidence X-ray diffraction (GIXRD) or small-angle X-ray scattering (SAXS), can provide information about surface nanotopography.
- **Scanning Electron Microscopy (SEM).** SEM utilizes a focused electron beam to scan the substrate surface that interacts with the surface, generating signals (secondary electrons, backscattered electrons or X-rays) that can be detected and used to create high-resolution surface topography images.
- **Transmission Electron Microscopy (TEM).** TEM involves transmitting a beam of electrons through a thin substrate and capturing the transmitted electrons to form an image.
- **Scanning Probe Microscopy (SPM).** SPM encompasses techniques like AFM, scanning tunneling microscopy (STM), and others. These techniques utilize a sharp probe that scans the substrate surface, measuring multiple physical properties such as surface topography, conductivity, or magnetic properties.

- **AFM.** AFM uses a sharp tip mounted on a cantilever to scan the substrate surface, measuring the interaction forces between the tip and the surface that can generate 3D surface maps, revealing nanoscale features and roughness.

Each technique has its advantages and limitations, and the choice of technique depends on factors such as the desired resolution, sample type, and specific experimental requirements. Researchers often employ a combination of techniques to gain a comprehensive understanding of nanotopography and surface characteristics.

The roughness measurements (both qualitative and quantitative) for nano-engineered implants are routinely performed via AFM [60,61]. AFM allows for thorough surface topography analysis of nano-engineered implants, including surface topography visualization, roughness, porosity and nanostructure dimensions. The AFM extracted information for nano-engineered implants, when compared with controls in a biological experiment (*in vitro* or *in vivo*), aids in linking surface topography to biological performance with cells or tissues. The following discusses key investigations utilizing AFM to characterize nano-engineered implant surface morphology and roughness:

Oyarzún et al. [62] optimized the use of AFM towards surface morphology characterization and thickness calculation of anodized titania nanopores (TNPs). Via the beam bounce and intermittent tuning fork configurations, the authors used AFM imaging of TNPs in contact mode; however, the beam bounce imaging did not appropriately characterize the 120 nm diameter TNPs. Tuning fork configuration yielded high-resolution imaging of the TNPs (Fig. 2). The observation is attributed to the advantages of an intermittent tuning fork over contact mode, including large spring constant, high sensitivity (both in amplitude and phase) and high mechanical quality factor [62]. Further, the mean radius values from AFM (57 ± 19 nm) were very similar to FESEM imaging (60 ± 15 nm).

Mathai et al. employed electrochemical deposition of hydroxyapatite on Ti implants via incorporating collagen peptide and polypyrrolle, followed by *in vitro* mineralization and bioactivity testing [63]. The bioactive polymeric nanocomposite coated Ti implants were characterized by AFM and revealed small globular domain-like rough morphology, with a thickness of the formed coating ~ 2 μm (analyzed from 3D AFM scan), that can augment implant-tissue integration.

Chico et al. used Nitrogen-ion implantation on AISI 304 austenitic stainless steel to perform surface modification, followed by optimization of the implant surface, implantation and thorough characterization via AFM [64]. Analysis of surface roughness and various superficial structures confirmed enhanced roughness (two-fold increase) post-ion implantation and the presence of pin holes attributed to ion bombardment (~ 3.2 μm wide and 14 nm deep).

To investigate if stainless steel's roughness and topography influence the initial attachment of dental-implant relevant bacterium *S. gordonii*, Chinnaraj et al. used AFM to model surface roughness via reconstruction of topography [65]. The influence of surface roughness and pattern in static and fluid flow conditions were investigated via computational modelling. Results revealed that rough surfaces (sub-micro scale) enhance bacterial attachment in static fluid conditions.

Implant nano-engineering not only alters surface topography but can also change the chemistry of the implant surface, and the precise influence of implant surface topography and chemistry on bioactivity needs to be better understood. In 2021, Guo et al. fabricated controlled nanotopographies on Ti implants via anodization with either similar topography or similar chemistry [55]. Combined SEM and AFM characterization confirmed the successful fabrication of controlled nano-engineered Ti, and bioactivity analysis showed that protein adhesion and gingival fibroblast proliferation are influ-

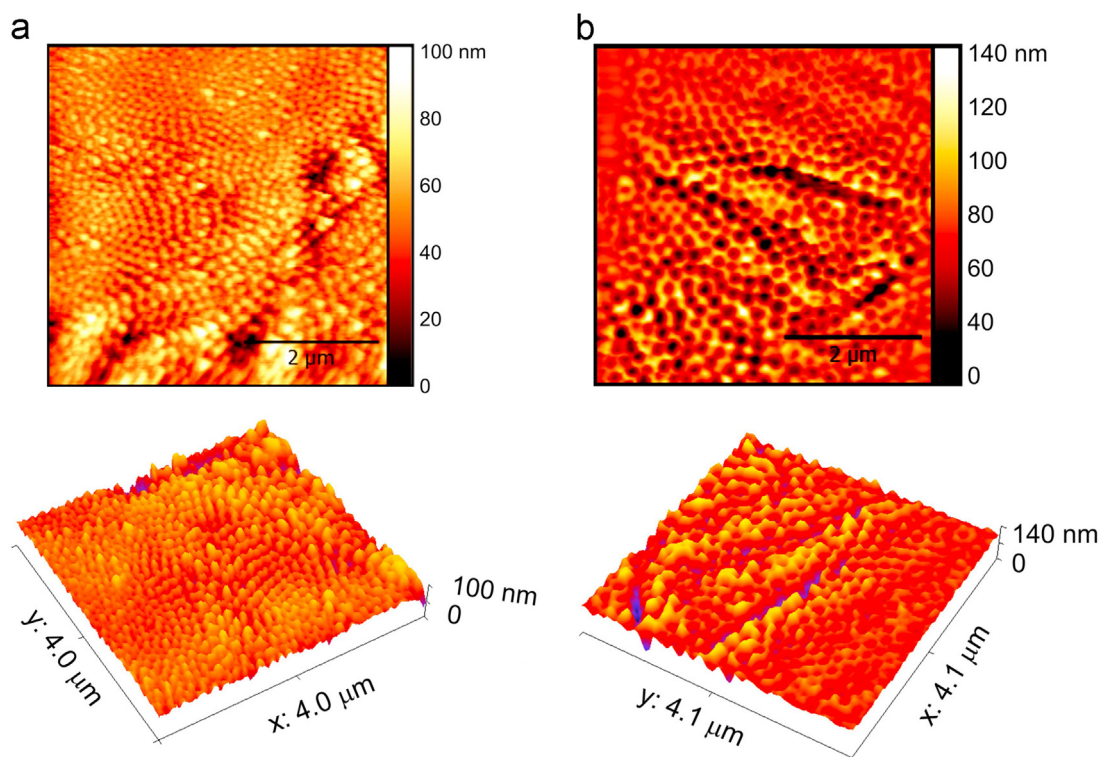


Fig. 2. Titania nanopore characterization using AFM. Imaging using (a) contact mode beam bounce configuration and (b) intermittent tuning fork configuration. Adapted with permission from [62].

enced by chemistry and topography. In contrast, cellular spreading and alignment are affected by surface topography.

AFM-based surface morphology and roughness measurements were used to characterize anodized dental implants that also provided details regarding the granular structure size of the anodized surfaces [66]. The 3D AFM imaging of anodized and bare implants exhibited varied surface morphologies and roughness quantifications, confirming that anodized implants were rougher and presented granules that can aid in promoting cell adhesion towards soft-tissue integration.

4.2. Mechanical characterization

AFM can also be utilized to measure and analyze the mechanical properties of materials at the nanoscale [67]. It allows for precisely probing surface topography and mechanical interactions between the AFM tip and the sample [15]. A mechanical map can be generated by acquiring force-distance curves at different locations on the sample surface, revealing variations in properties such as surface roughness, stiffness, elasticity, and adhesion [68]. Surface roughness is quantified by measuring the height variations across the sample surface. Stiffness and elasticity can be determined by analyzing the slope or indentation depth in the force-distance curves. Further, adhesion forces can be obtained by analyzing the force required to detach the tip from the surface. Additionally, AFM can be combined with other techniques, such as lateral force microscopy (LFM) and friction force microscopy (FFM), to study frictional properties and surface interactions and provide insights into tribological properties, surface friction, and wear characteristics. Mechanical characterization using AFM offers valuable information for understanding material behavior, assessing mechanical properties, evaluating coating adhesion, and studying surface interactions at the nanoscale [69].

Kim et al. compared the mechanical performance of Silicon nanowires characterized via AFM bending and nanoindentation testing and concluded that AFM bending (based on the line tension model) is the most favorable and reliable characterization technique for Silicon nanowires [70]. Similarly, AFM has been used to measure the mechanical properties of ceramic nanowires (potassium-stabilized manganese dioxide nanowires) [71], gold nanowires [72] and electrospun poly(L-lactide) fibres [73].

Bypassing multi-step specimen preparation and modification needed for conventional mechanical testing and SEM imaging, Angeloni et al. reported the use of contact mode imaging (CMI) and force spectroscopy imaging (FSI) methods of AFM to quantify mechanical characteristics of as-fabricated micro- and nanopillars [74]. The nanopillars were additively manufactured using two-photon polymerization (2PP) and electron beam-induced deposition (EBID), and using AFM, various characteristics, including stiffness, failure stress, adhesion force, maximum lateral force and maximum deflection were measured. Both AFM-based methods yielded similar results, and the proposed methods can allow for mechanical measurements, especially when tested in wet conditions, for example, nanopatterned implant surface for mechanobiological investigations.

In 2022, Wood et al. reported nanomechanical tribological characterization of hydrothermally-etched (HTE) nano-engineered titanium alloy surfaces using AFM [75]. The authors used AFM in Lateral Force Microscopy mode to investigate the contact friction between orthopedic implants and local tissue. The contact behaviour between a smooth alloy and HTE surfaces against a hardwearing SiO₂ sphere was simulated. Friction investigation (both in air and liquid environments at varied velocities) revealed that friction on the HTE surface was reduced by ~20% (air) and ~80% (liquid). Hence, reduction in friction can augment wear resistance and help achieve implant-bone integration.

Contact resonance AFM uses the cantilever's contact resonance frequency and quality factor values to characterize mechanical properties, including elastic modulus and loss tangent of the specimen. However, it is associated with a limitation – a time-consuming frequency sweep that makes quantitative scanning impractical. To address this challenge, in a recent study, Yang et al. reported a cantilever design with an integrated inner-paddle substructure that keeps the resonance consistent [67]. This enhanced probe enables fast single-frequency amplitude imaging to measure the elastic characteristics of the specimens.

4.3. Chemical Characterization

AFM-Chemical Force Spectroscopy (AFM-CFS)

AFM can be used for Chemical Force Spectroscopy (CFS), a specialized mode of AFM that enables the measurement of chemical interactions between a probe tip and a sample surface [76]. In AFM-CFS, the cantilever probe is functionalized with specific chemical groups or molecules that can selectively interact with the target molecules on the sample surface. The basic working principle of AFM-CFS involves bringing the functionalized cantilever probe into contact with the sample surface and then measuring the interaction forces as the probe is pulled away [77]. The cantilever deflection is recorded as a function of the vertical distance between the probe and the sample surface, generating a force-distance curve. This curve provides information about the strength and nature of the chemical interactions between the probe and the surface [78].

By analyzing the force-distance curves, AFM-CFS allows the quantification of various chemical interactions, such as receptor-ligand binding, antibody-antigen interactions, DNA hybridization, or enzyme-substrate interactions. The technique provides valuable insights into molecular recognition, binding affinities, and the kinetics of chemical reactions at the nanoscale. AFM-CFS has applications in various fields, including surface chemistry, biophysics, and materials science. It offers a powerful tool to investigate and understand molecular interactions and surface properties with high spatial resolution and force sensitivity. For biomedical applications, CFS has been used to evaluate biotin-streptavidin binding [79], hydrophobic/hydrophilic interactions [78] and hydrogen bonding in DNA bases [80].

AFM coupled with Infrared Spectroscopy (AFM-IR)

To analyze the chemical composition and changes at a nanoscale surface, AFM has been combined with infrared spectroscopy (AFM-IR) [81,82,83]. Briefly, AFM-IR measures the volumetric expansion of a material heated by a laser operating in the infrared range [84]. AFM-IR exceeds the diffraction limit of IR and probes IR absorption characteristics at the nanoscale [85] and can provide spatial resolution of AFM combined with IR's chemical characterization and compositional imaging ability. For example, Liu et al. used AFM-IR to observe the spatial distribution of oxygen functional groups on monolayer and multilayer graphene oxide (GO) [82].

4.4. Electrical characterization

Combining AFM with electrical measurements makes it possible to investigate charge transport mechanisms, carrier mobility, surface charge distribution, and electrical properties of nanostructures and device. This allows for the characterization and evaluation of electrical properties at high spatial resolution, providing insights into the functionality and performance of materials and electronic devices. Electrical characterization using AFM is widely used in various fields, including semiconductor research, nanoelectronics, photovoltaics, and materials science. It provides an understanding

of electrical behavior at the nanoscale, optimizing device performance, and developing new electronic materials and devices [86]. Studying electrical properties is crucial for biomedical/implant-related applications as the dielectric and piezoelectric forces influence the structural/functional characteristics of tissues, biomembranes and biomolecules [87]. In 2019, Cheong et al. extensively reviewed the application of functional AFM to measure electrical properties in biological applications [88]. The following describes the various modes of AFM to study the electrical properties of specimens:

Kelvin Probe Force Microscopy (KPFM)

AFM-based electrical characterization involves the measurement and analysis of electrical properties of materials at the nanoscale to investigate various electrical phenomena, including surface potential mapping, current-voltage characteristics, and charge transport [89]. One such technique is Kelvin Probe Force Microscopy (KPFM) which measures the local surface potential of a material by utilizing the contact potential difference between the AFM tip and the substrate surface [90]. The AFM tip (a probe electrode) scans the substrate surface while a feedback loop maintains a constant potential difference between the tip and a reference electrode. The resulting surface potential map provides information about the sample's local electrical properties and variations. KPFM enable characterization of nanoscale electronic or electrical characteristics of metals or semiconductor surfaces and semiconductor devices [90], and has also been utilized to evaluate electrical characteristics of organic devices [91] and biological specimens [92,93]. For example, KPFM has been applied to characterize protein-protein interactions [94], imaging individual DNA molecules on surfaces [95]. In 2016, Lee et al. reviewed the use of KPFM to analyze the surface potential of nanoscale biomaterials and devices, including various nanomaterials (nanoparticles, 3D layered nanomaterials, oligonucleotides) and nanomolecules for biosensing [96].

Conductive AFM (CAFM)

An alternative technique is Conductive AFM (CAFM), which measures the current-voltage (I-V) characteristics of a material at the nanoscale [97]. In CAFM, a conductive AFM tip is used to apply a bias voltage to the substrate surface, and the resulting current flowing through the tip-sample junction is measured. This technique enables the analysis of electrical conductivity, resistivity, and current distribution of materials, including semiconductors, conductors, and insulators. CAFM has been utilized to investigate electron transfer and conductivity properties of DNA, bacteria and biomembranes via recording current images and enabling quantitative I-V measurements [98,99].

Electrostatic Force Microscopy (EFM)

EEM measures the electrostatic force gradient between a substrate surface and the tip, providing crucial information on charge density, distribution, mobility and polarization. EFM can be used to characterize a wide variety of specimens, including organic nanorings and nanorods [100], natural macromolecules like DNA (assessment of localization and delocalization of charges) [101] or bacterial pili (charge propagation) [102].

Piezoresponse Force Microscopy (PFM)

PFM detects the electromechanical surface deformation and displacement induced by bias [103]. Local electromechanical characteristics such as surface deformation at the nanoscale induced via piezoelectric effect can be quantitatively measured [104]. For example, the piezoelectric response of natural tissue mimicking self-assembled fluorenylmethyloxycarbonyl diphenylalanine (Fmoc-FF) nanotubes and nanofibrils (applied as tissue engineering scaffolds) has been studied using PFM [105]. The piezoelectricity of Fmoc-FF fibrous networks holds great promise in biomedical applications involving electrical or mechanical stimuli. Further, electromechan-

ical properties of collagen fibrils [106], amyloid fibrils [107], bacteriophage [108], ECM protein elastin [109] or biological tissues (bones, brain, tendons, etc.) [110,111] have also been studied using PFM.

Scanning Electro-Chemical Microscopy (SECM)

Belonging to the Scanning Probe Microscopy (SPM) family, the development of ultramicroelectrodes and Scanning Tunneling Microscopy (STM) has yielded the result of SECM. Briefly, the SECM working principle is based on accurate tracking and monitoring of the 3D movement of the probe on the specimen via the piezoelectric actuator [112,113]. SECM can enable studying enzymes' catalytic activity and kinetic parameters via feedback or generation collection modes. SECM has been applied to study molecular configuration and hybrid information of DNA [114], the kinetics of enzymes immobilized on biosensors [115] and cellular topography [116].

4.5. Magnetic force microscopy (MFM)

MFM is a specialized imaging technique that combines the AFM working principle with magnetic sensing capabilities and allows for the visualization and characterization of magnetic properties at the nanoscale [117]. It provides information about a material or substrate surface's magnetic field distribution, magnetic domains, and domain walls.

A conventional AFM tip is replaced with a magnetic-coated probe tip in MFM. The magnetic tip interacts with the magnetic field radiating from the substrate surface, and the resulting magnetic forces are detected and measured. As the probe scans the substrate surface, the magnetic forces vary depending on the local magnetic properties, creating a topographic image with simultaneous magnetic contrast [118].

Enabling the visualization of magnetic domain structures, domain sizes, and their interactions, MFM can provide valuable insights into materials' magnetic properties (ferromagnetic, paramagnetic and antiferromagnetic behaviors) [119,120]. As a result, MFM is widely used in materials science, magnetism research, data storage, and spintronics. For example, MFM enables the characterization of ultrathin magnetic films (Ag/Fe/Ag) [121] or superconducting Nb films [122].

4.6. AFM tip-based nanomanufacturing (TBN)

AFM-TBN is a technique that utilizes the sharp tip of an AFM probe to manipulate and fabricate nanostructures with high precision [123,124]. The process involves bringing the AFM tip into contact with a material surface and applying controlled forces or electrical potentials to induce specific nanoscale modifications. This can include nanolithography, nanomanipulation, nanodisplacement, or nanoscale deposition. By carefully controlling the motion and forces exerted by the AFM tip, it is possible to create intricate patterns, manipulate individual atoms or molecules, or fabricate nanostructures with tailored properties. TBN can fabricate micro/nanostructures via mechanical removal, such as grooves, dots/lines or 3D structures on flat and curved substrate surfaces [125]. Besides, mechanical-chemical and mechanical-thermal effects from AFM can also enable controlled micro/nano-engineering [126]. In 2003, Agarwal et al. reported the use of AFM probes to chelate poly-histidine-tagged peptides/proteins and free-base porphyrins onto ionized regions of nickel surface via the application of an electric potential to the AFM tip [127]. AFM-TBN offers excellent potential for nanoelectronics, nanophotonics, and nanomedicine applications, enabling the precise fabrication of functional devices and structures at the nanoscale.

4.7. Evaluating nanoparticle interaction

Silver nanoparticles (NPs) and ions are potent bactericidal agents that have been used across various applications, including biomedical implants (for instance, loaded inside anodized Ti with nanotubes for local therapy); however, concerns remain over its dose-dependent cytotoxicity [128,129]. Further, other metallic or polymeric NPs have been used to enhance bioactivity and local therapy from modified implants [130]. However, investigations are needed to better understand NPs interaction, internalization and cytotoxicity with tissue-resident cells.

To shine a light on the aquatic cytotoxicity of Ag NPs and their detoxification via diatom algae, Pletikapić et al. used AFM to investigate Ag NPs' interaction with algal cells' extracellular polymeric substance (EPS), dependent on its size, shape and structure [131]. Citrate-stabilized Ag NPs were synthesized and interacted with marine diatoms *Cylindrotheca fusiformis* and *Cylindrotheca closterium*, and their EPS was characterized via AFM to reveal NPs internalization and detoxification mechanism. Ag NPs induced morphological alterations and structural damage to the cells was studied via AFM (use of contact mode to scan the entire cell). While untreated cells had easily recognizable cellular features, the Ag NPs-treated cells showed clear evidence of moderate to high damage. Next, to evaluate NP-cell wall interaction, high-resolution AFM was performed. Again, Ag NP treatment resulted in a deformed surface and attachment/penetration of NPs, resulting in pits (Fig. 3). Evidence of Ag NPs attachment as individual particles or clusters (average height of 30–40 nm) on the cellular valve region is confirmed (Fig. 3a). Smaller NPs were detected in the girdle band and valve (Fig. 3d). Further, pore-like lesions or pits (100–160nm wide and 30nm deep) were visible on the valve region (Fig. 3b-d). These observations confirm that the pits are NP penetration sites and indicate that NPs cross the cell wall.

While the abovementioned study did not directly relate to NP-modified or NP-releasing implants, it provides evidence that AFM can be utilized to examine the internalization of NPs (released from the implant surface) into the cells. This, in turn, can aid in predicting the uptake of therapeutic NPs by cells or cytotoxicity, thereby providing information on implant bioactivity.

Several other attempts have been performed to investigate nanoparticle toxicity. Vasir et al. used AFM and confocal microscopy to study the interaction of Poly(D,L-lactide-co-glycolide) (PLGA) NPs functionalized with poly-L-lysine [132]. The findings revealed that functionalized NPs have a 5X higher adhesion force with the cell membrane, and time-lapse AFM imaging confirmed rapid internalization compared to unmodified NPs. Next, Rai et al. studied the antimicrobial effect of antibiotic-functionalized Au NPs (52–22 nm), and combined FTIR/AFM analysis revealed that the NPs' antimicrobial activity against Gram-positive (*Staphylococcus aureus*) and Gram-negative (*Escherichia coli*) bacteria results from antibiotic inhibition of peptidoglycan layer synthesis and Au NPs causing cell death via generation of 'holes' in the bacterial cell walls [133]. Shukla et al. have also explored the biocompatibility and endocytotic fate of Au NPs inside RAW264.7 macrophages using AFM and reported that NPs' internalisation happens via the pinocytosis mechanism [134]. Further, Potara et al. fabricated Ag NPs capped in chitosan and studied bactericidal efficacy against *Staphylococcus aureus*, and AFM analysis confirmed bacterial cell wall disruption upon incubation with chitosan-Ag NPs [135].

In summary, AFM allows for examining cellular morphology in response to NPs exposure, which provides information on NPs internalization or cytotoxicity. Since NPs offer exceptional bioactivity and therapeutic functionalities and are emerging as modification strategies for nano-engineered implants, NP-releasing implants can be tested via AFM.

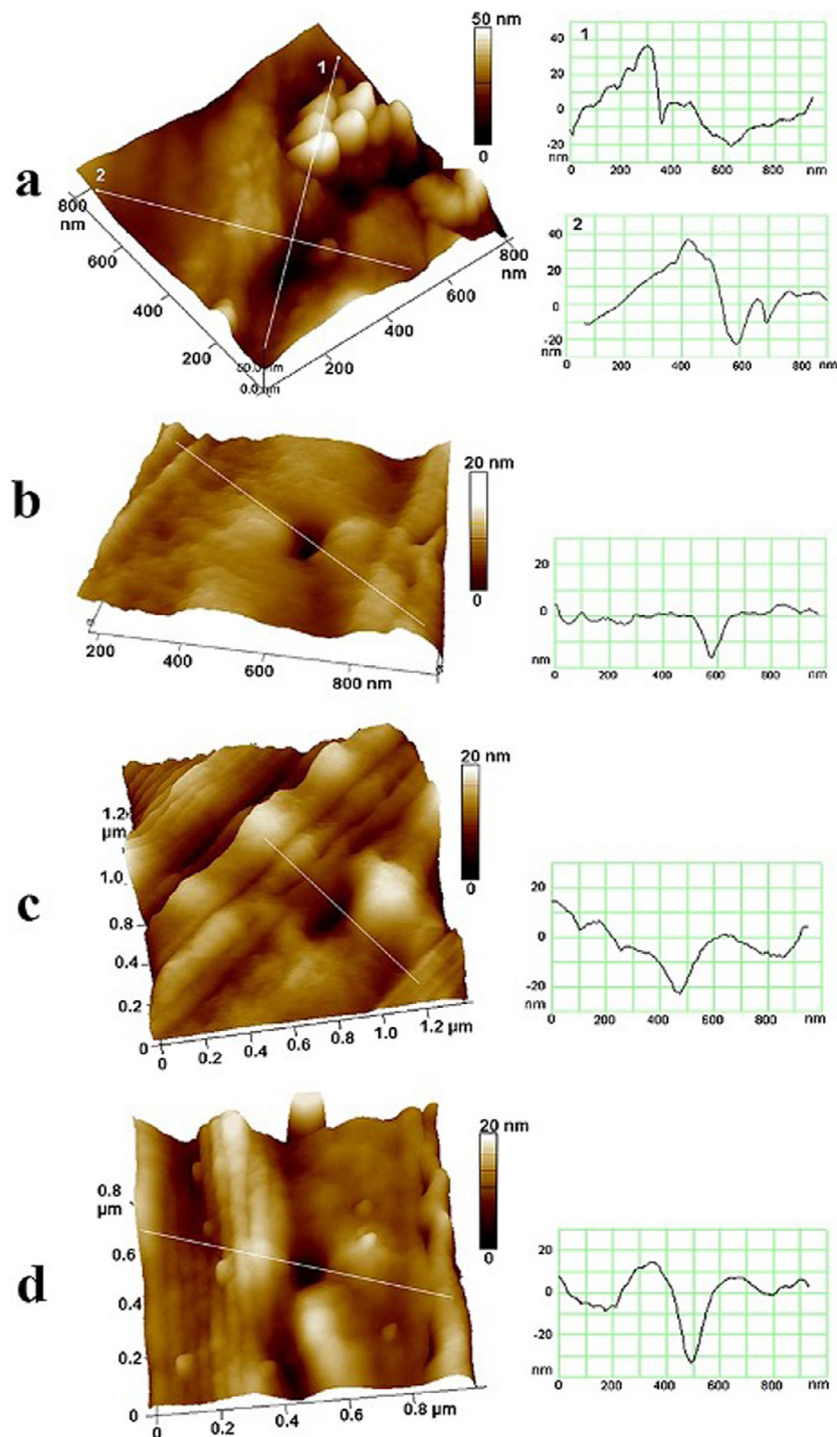


Fig. 3. Nanoparticle toxicity evaluation. AFM imaging of *Cylindrotheca fusiformis* cell walls after 24 h exposure to 10 mg/l Ag NPs. Adapted with permission from [131].

5. Single-cell force spectroscopy (SCFS)

5.1. Basics of SCFS

SCFS is a technique that measures and analyzes the mechanical characteristics of individual cells. Briefly, it involves the application of controlled mechanical forces to a single cell and monitoring the resultant responses of the cell [136]. SCFS provides crucial information into cellular mechanics, including adhesion, deformability, stiffness and interactions with a substrate. In simple terms, SCFS involves using a microscale-sized probe, for instance, an AFM

cantilever or an optical trap, to apply controlled forces onto a cell [137]. The technique permits precise manipulation via the application of various magnitudes and durations of forces. As a result of the applied force, the probe is deflected, or the cell is displaced.

SCFS allows users to measure cellular characteristics at a single-cell level. For cell-substrate interactions, SCFS can measure the forces required to detach cells from the substrate or investigate the influence of external forces on cell-substrate adhesion. Besides, SCFS can also be utilized for cell membrane mechanics (tension, rupture forces or elasticity), cell-extracellular matrix (ECM) interactions, cell-cell adhesion (interactions between cell surface recep-

tors and their ligands), or cellular stiffness (force required to deform a cell).

SCFS outcome can be used to construct force-distance curves that provide a quantitative representation of the forces experienced by a cell as a function of the applied probe displacement. Analysis of f-d curves enables the extraction of mechanical parameters and characterizing cell behavior under various conditions. SCFS applications span multiple fields, including biomechanics, tissue engineering, cell biology and biomedical research. SCFS can improve our understanding of cellular responses to mechanical cues and disease-related changes in cellular mechanics [138].

5.2. SCFS techniques

Various techniques can provide multiple means to apply and measure forces on single cells. Choice of technique influences the specific experimental requirements, desired force range and spatial resolution. Each SCFS technique has its advantages and shortcomings, and researchers often select the most suitable technique based on instrument availability, expertise and research goals.

Optical Tweezers. Also known as laser traps, they utilize focused laser beams to trap and manipulate microscopic objects (such as cells). By using the gradient forces of the laser beam, optical tweezers can apply controlled forces to a single cell and the displacement of the trapped cell can be measured to assess its mechanical response [139].

Magnetic Tweezers. These use magnetic fields to manipulate and exert forces on magnetic particles attached to cells [140]. By controlling the magnetic field strength and direction, precise forces can be applied to the cell, and the resulting cellular displacement/deformation is measured.

Micropipette Aspiration. It involves using a glass micropipette to aspirate a single cell into the pipette, and by applying suction to the pipette, controlled forces can be exerted on the cell [141]. The degree of deformation or the pressure required to aspirate the cell provides information about its mechanical properties.

Computer-Controlled Micropipette. It is a micropipette system that is controlled by a computer. The computer-controlled system allows for precise force control, recording of force-distance curves and real-time data analysis.

Microfluidics. Various microfluidic techniques, such as microfluidic stretching, hydrodynamic forces, or shear flow, offers precise control over fluid flow and enable the application of controlled forces to individual cells that can be utilized to assess the mechanical properties of cells.

Microneedle Manipulation. Glass or quartz microneedles mechanically interact (push, stretch, or indent) with a single cell, and the resulting forces and deformations are measured to evaluate the cell's mechanical response.

Atomic Force Microscopy (AFM). It is one of the most widely used SCFS techniques and involves using a sharp tip mounted on a cantilever to probe the mechanical properties of cells. The tip interacts with the cell surface, and the resulting deflection of the cantilever is measured, providing information about the forces experienced by the cell.

Fluidic Force Microscopy (FluidFM). It combines the capabilities of an AFM with localized fluid delivery and aspiration [142]. It involves integrating a hollow cantilever probe with microfluidic channels to enable precise fluid manipulation at specific locations on a substrate surface. FluidFM can allow for the controlled delivery of liquids (drugs or nanoparticles) to targeted areas and aspiration of liquids from specific regions. Using FluidFM, localized experiments such as single-cell manipulation, chemical patterning, or controlled deposition of molecules can be performed [32].

Robotic Fluidic Force Microscopy (Robotic FluidFM). Integration of FluidFM technology with a robotic systems is called Robotic Flu-

idFM. Combining FluidFM's precise fluidic manipulation capabilities with the robotic platform's automation and control enables high-throughput and systematic experimentation by automating the processes (probe alignment, sample positioning, fluid delivery and data acquisition) [143]. Enhancing the efficiency and reproducibility of FluidFM, Robotic FluidFM can be applied towards large-scale screening, high-resolution imaging, and manipulation of multiple specimens.

Ultrasonic. Employing ultrasonic waves, this technique assesses the strength and properties of cell adhesion. Briefly, a cell-substrate or cell-cell adhesion interface is subjected to ultrasonic vibrations, and then the resultant changes in frequency, amplitude, or energy reflection are measured. The ultrasonic waves induce mechanical stress at the adhesion site, causing cell detachment or deformation.

5.3. SCFS via atomic force microscopy (AFM)

SCFS via AFM systematically applies and measures forces that enable the investigation of individual cells' mechanical properties with high spatial resolution, thereby providing critical information about cellular mechanics, adhesion and responses to external mechanical stimuli [137,144,145]. The working principle of SCFS via AFM involves:

Probe Preparation. A cantilever tip (or probe) is prepared for the experiment via functionalization with specific molecules.

Approach. Probe is positioned on the cell of interest and the cantilever is gradually brought closer to the cell surface. AFM's feedback mechanism system maintains a constant force or deflection during the approach phase.

Contact. Upon contact with the cell surface, a minute contact force is applied and the cantilever deflection (resulting from the mechanical properties of the cell) is measured. This deflection can be used to calculate applied force.

f-d curve. Upon retraction of the probe, f-d curve is recorded that represents the mechanical response of the cell to the applied forces.

Analysis. The curve can be divided into regions corresponding to different cellular events, such as cell adhesion, cell-substrate detachment, or membrane rupture that can be analyzed to extract various mechanical characteristics of the cell. Further, parameters like cell stiffness or adhesion force can be calculated via curve fitting to appropriate models.

Repeat. The process is repeated under different experimental conditions and for multiple cells to extract statistically relevant data.

5.4. Cantilever functionalization

A cantilever must be functionalized with a cell-adhesive reagent to ensure the successful fishing of a single cell. Preparing the cantilever of an AFM for attaching cells in SCFS generally involves:

Cantilever Cleaning. Functionalization procedures generally involve cleaning cantilevers with one or combined strategies: chemical treatment (sulfuric acid or acetone), UV irradiation and/or plasma cleaning [146] to ensure a pristine surface.

Cantilever Functionalization. Summary of key functionalization methods utilized to modify the cantilever for SCFS [147]:

Lectins (common plant lectin, Concanavalin A, purified from jack beans): binds to mannose residues of glycoproteins and is the most commonly used functionalization method [146,148–151]; however, can cause alterations in cell stiffness.

Streptavidin (binding to biotinylated cells): well known and understood, attributed to its high affinity as a noncovalent bond that is often used to couple molecules [152,153].

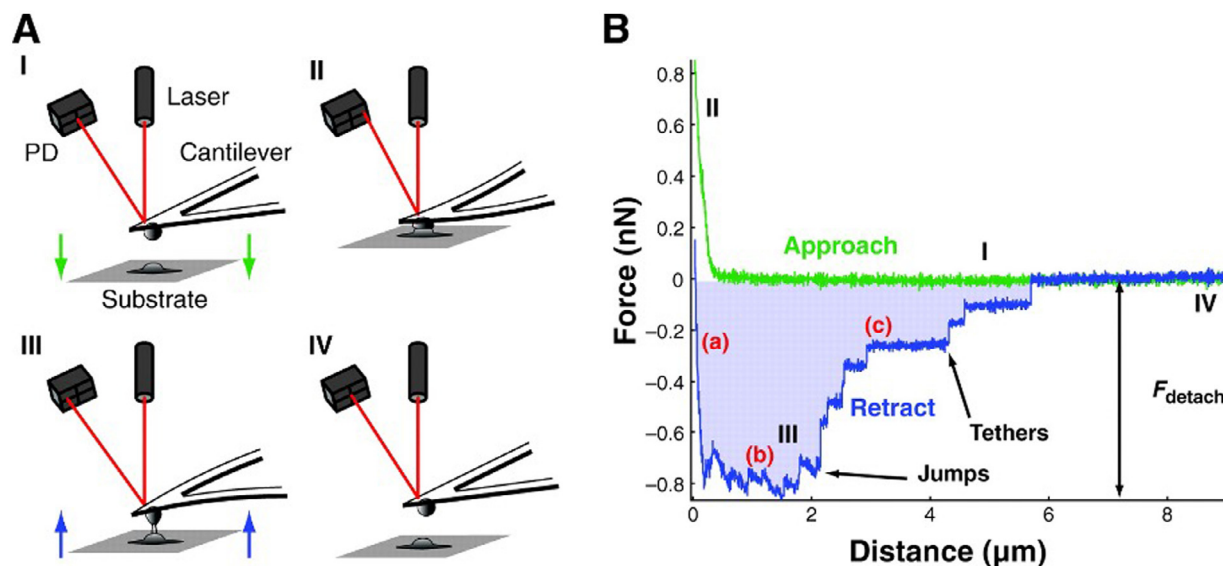


Fig. 4. SCFS via AFM. **A.** SCFS working principle, representation of cell adhesion measurement. Green arrows: approach; blue arrows: retract [corresponds to force vs distance curve in (B)]: **A-I:** Contact between substrate and cell. Cantilever (CL) deflection and the force that acts on CL are measured by the laser beam (red) position on the photodiode (PD). **A-II:** Cell is pressed (approach) onto substrate until a pre-set force is reached. **A-III:** After a predetermined contact time, the cell is retracted, yielding the F-d curve (B). **A-IV:** Complete cell detachment. **B.** Force vs. distance graph showing jumps, tethers and the detachment force, characteristic of a force signature. Attributed to an increase in strain on the cell, the bonds between cell-substrate break sequentially (A-III) until the complete separation of the cell is achieved (A-IV). F_{detach} is the maximum downward force experienced by the CL. In cell-substrate separation, two molecular unbinding events occur. *Jumps* (with a decrease in force magnitude, receptor remains anchored in cell cortex and unbinds); and *Tethers* (loss of receptor anchoring and pulling out of membrane tethers, characterized by the long plateau of constant force or pulling distance of several μm s). (a-c) in B denotes varied phases of cell-substrate detachment. Adapted with permission from [21].

ECM proteins (like fibronectin): bind to cell-adhesion receptors and can modulate cells' adhesive characteristics.

BD CellTak (polyphenolic protein from marine mussels): cell and tissue adhesive that is commercially available and can be used to attach cells/tissues to glass, plastic, metals or polymers.

Pressure-controlled cell capture: Underpressure is applied via microfluidic channels in the cantilever to immobilize cells, allowing for sequential capture of multiple cells using the same cantilever. However, the technique requires specific instrumentation.

Verification. The successful attachment of the functional molecules onto the cantilever is confirmed using fluorescence microscopy or other labeling methods to visualize the presence and distribution of the attached molecules on the cantilever surface.

Cell Attachment. Before SCFS experiments, the cells are introduced onto the functionalized cantilever surface. The cells may adhere via specific receptor-ligand interactions or non-specific adhesion forces.

SCFS Experiment. During the SCFS experiment using the functionalized cantilever with attached cells, the desired force protocols are applied, followed by measurement of the forces between the cantilever and the cell and analysis of the resulting data.

5.5. Understanding force-distance curves

Taubenberger et al. [147] have performed an extensive review of the use of AFM-SCFS as a tool to quantify cellular adhesion onto implants. During the separation of the cell from the substrate, the cantilever deflects proportionally to the vertical force between the cell and substrate, which yields the characteristic force-distance curve that provides the cell adhesion signature. Overall, the force-distance retrace curve can be broken into three phases, as described by Helenius et al. [21] (Fig. 4, Table 1). Briefly, after the contact is established between the cell and the substrate for a predetermined time, the cantilever is retracted to detach the cell. During this detachment, the force acting on the cantilever (detachment force or F_{detach}) is recorded by the distance (d) travelled by cantilever in the force-distance curve (F-d curve). F_{detach} is the maxi-

mum detected force when the cell is separated from the implant surface. Contact force, time and height and cantilever pulling velocity are critical determinants of the F-d curve [147]. The resultant curve displays the specific and complex force patterns characteristic of the cell-substrate interaction and is referred to as the force signature.

5.6. Factors influencing SCFS outcomes

The SCFS experiment permits excellent control over the parameters that can significantly influence the experimental outcome [147].

Applied Contact Force. It is established that high contact force increases detachment forces [147,156] which is attributed to the deformation of the viscoelastic cell body under the influence of the applied force that increases the apparent cell-substrate contact area.

Substrate Roughness. Substrate roughness can have a significant influence on AFM-SCFS outcomes:

Adhesion Strength. Substrate roughness can affect the adhesion strength between the cell and the substrate. Increased roughness can provide more surface area for cell-substrate contact, enhancing adhesion forces [157]. Conversely, a smoother substrate may result in reduced adhesion forces. The roughness-induced variations in adhesion strength can influence the force measurements and the observed interaction between the cantilever and the cell.

Contact Area and Distribution. Substrate roughness can alter the contact area and distribution of forces between the cell and the substrate. In the presence of roughness, cellular processes (filopodia or microvilli) can conform to the substrate topography, resulting in localized contact regions, leading to variations in the distribution of forces during SCFS experiments and affecting the data interpretation.

Mechanical Strain. As the cantilever moves over the rough surface, the cells experience varying levels of mechanical stress due to the changing local topography. This strain can influence cellular responses and alter the measured forces.

Table 1

The three phases of the force-distance retrace curve (or cell-substrate detachment) and the involved forces.

Phases	Events and forces involved	Events at cell-substrate adhesion points
(i)	Cantilever pulls the cell, and as the pulling force increases, force at the cell-substrate adhesion interface increases. Dependent both on cell (elasticity, cortex tension, geometry) and receptor (binding strength, placement) characteristics [21].	Mechanical deformation of the cell cortex
(ii)	Cell detachment from the implant surface. Individual force steps.	Receptor detaches from the substrate or pulled away from the cell cortex
(iii)	Cell contact with the implant surface ends. Attachment is mediated by tether attachment [154,155].	Cell completely detached from the implant surface

Measurement Artifact. The presence of surface features or irregularities can affect the contact mechanics between the cantilever and the cell, leading to uncertainties in the force measurements. Further, roughness-induced vibrations or noise can interfere with the accuracy and reliability of force spectroscopy data.

Spatial Resolution. The rough features on the substrate can limit the ability to precisely position the cantilever tip on specific cellular regions of interest. This can affect the ability to probe localized adhesion forces or perform targeted force measurements on specific cell structures.

Cell-Substrate Contact Time. As the contact time increases, the number of cell receptors interacting with the substrate increases, enhancing the detachment force. While a free-moving cell needs several minutes to establish high-order adhesion sites, for AFM-SCFS, small integrin clusters have been observed within one minute of contact [158,159]. It is noteworthy that further increased contact times can lead to high-strength adhesive interactions between cell and substrate, which can outperform cell-cantilever strength and damage the cell upon cantilever retraction.

Cantilever Retraction Speed. During cell detachment, the cantilever retraction speed determines the loading rate at which the adhesive bonds are stressed. Further, the nature of the bond and the range of applied loading rates dictate if the bond lifetime will increase or decrease [160,161]. Hence it is recommended that the retraction speed is kept constant when the adhesion of various cell types is compared. Notably, changes in cantilever retraction speed can influence the force-distance curve.

Cell Elasticity. The abovementioned represent experimental settings and substrate surface characteristics that can easily be controlled. Other contributing factors, including cellular elasticity, are beyond instrument settings and can significantly influence the contact area between the cell and the substrate surface. Hence, cells with similar elastic characteristics should be used for a study. Additionally, cellular morphology and viability can be visualized by combining SCFS with confocal/fluorescence microscopy [162].

Cantilever functionalization. The choice of functionalization method and the functional molecules (including lectins, streptavidin, ECM proteins, BD CellTak or pressure-controlled cell capture) attached to the cantilever can significantly impact the interactions between the cantilever and the cell, thereby influencing the SCFS measurements and outcomes, as detailed next:

Specific Interactions. The specificity of cell-substrate interactions ensures that the force measurements are specifically related to the interactions of interest and reduces non-specific interactions with the substrate or other cellular components.

Adhesion Strength. The choice of functionalization can influence the strength of adhesion between the cell and the cantilever, which affects the magnitude of the measured forces during SCFS experiments. Modifying the cantilever surface enables control over the adhesion strength and tailors the measurements to the desired force range.

Cell-Cantilever Interaction Stability. Proper functionalization ensures the cell remains attached to the cantilever throughout the

measurement process, allowing for accurate and reliable force measurements over time.

Detection and Sensitivity. Cantilever functionalization with suitable molecules can enhance the detection and sensitivity of SCFS experiments. For instance, using functionalized nanoparticles or specific surface coatings, the signal-to-noise ratio can increase, allowing for more precise force measurements and improved quantification of cellular interactions.

Cellular Functionality Preservation. The functionalization should not negatively affect the cell viability, morphology or mechanical properties, as this could introduce artifacts and compromise the accuracy of force measurements.

Cantilever characteristics. The characteristics of the cantilever in AFM-SCFS, including its geometry and stiffness, significantly influence the outcomes of the experiments. Following are some ways in which cantilever characteristics affect AFM-SCFS outcomes:

Force Sensitivity. Cantilever stiffness determines its sensitivity to applied forces. A stiffer cantilever will deflect less for a given force, providing higher force resolution and enabling the measurement of smaller forces. Conversely, a more compliant cantilever will deflect more for the same force, allowing for the measurement of larger forces. The choice of cantilever stiffness is based on the expected range of forces involved in the specific SCFS experiment.

Spring Constant. The spring or stiffness constant, quantifies the relationship between the cantilever deflection and the applied force, and influences the calibration/accuracy of force measurements in AFM-SCFS. Higher spring constants provide higher force sensitivity and better resolution for measuring small forces, while lower spring constants are suitable for measuring larger forces.

Cantilever Geometry. The geometry of the cantilever (length, width, and shape) affects the force distribution and the mechanical properties of the cantilever. It influences the contact area between the cantilever and the cell, affecting the spatial resolution and the ability to probe specific cell surface regions.

Resonance Frequency. Dependent on cantilever geometry and stiffness, resonance frequency also impacts the dynamics of force spectroscopy experiments. It determines the frequency at which the cantilever oscillates when excited by a driving force. Appropriate selection of the resonance frequency allows for efficient and accurate force measurements by avoiding interference from the environment.

Tip Properties. The shape, radius, and material characteristics of the tip attached to the cantilever can influence the force distribution, spatial resolution and the ability to probe specific cellular features. An appropriate tip ensures suitable contact with the cell surface to minimize potential damage or deformation.

Time of Measurement. The time of measurement, specifically the duration between cellular attachment to the cantilever and the initiation of AFM-SCFS measurements, can have an impact on the experimental outcomes, as described next:

Cell Adaptation. After attachment to the cantilever, cells require time to adapt and adjust to the mechanical and biochemical cues of the cantilever surface. The duration of this adaptation phase can vary depending on the cell type and experimental conditions. It

is crucial to allow sufficient time for the cells to settle and reach a stable state before starting the force measurements. Premature SCFS measurements can yield inconsistent or unreliable data due to incomplete cellular adaptation.

Cell Spreading and Morphology. Depending on the nature of the experiment and the desired cellular response, the time of measurement can affect cell spreading and attachment stability. The extension of cellular processes, such as lamellipodia or filopodia, and the establishment of cell-substrate contacts can affect the mechanical response during force measurements. The time of measurement can influence the extent of cell spreading, cell-substrate interactions, and the resulting force profiles.

Cellular Responses and Adaptation. Cells can exhibit time-dependent responses to their mechanical environment. For instance, cells may gradually remodel their cytoskeleton or alter their adhesion properties in response to external forces. The time of measurement can influence the cellular response, including changes in cell stiffness, adhesion strength, or the formation of cellular structures involved in force transmission. Performing measurements at different time points allows for the investigation of time-dependent cellular responses.

Cell Viability and Health. The viability and health of the attached cells can be affected over time, as the cells may experience changes in metabolic activity, viability, or physiological status during prolonged measurements. It is crucial to consider the time of measurement to ensure that the cells remain viable and representative of their physiological state. Prolonged measurements could potentially lead to cellular stress or changes in cellular behavior that may affect the obtained force data.

Biological Processes and Dynamics. The time of measurement can also relate to specific biological processes or dynamics under investigation. For example, if the experiment aims to study the kinetics of cellular adhesion or the response to a specific stimulus, the time of measurement becomes a critical influence.

5.7. Stresses faced by a single cell during SCFS

During AFM-SCFS, single cells experience various types of stresses that can alter their behavior and properties:

Mechanical Stress. AFM-SCFS applies mechanical forces to the single cell through the cantilever probe and these forces can deform or displace the cell membrane, leading to mechanical stress on the cell.

Adhesion Stress. AFM-SCFS measures the adhesion forces between the cell and the substrate or nanostructure. The process of probing adhesion forces can induce stress on the cell-cell or cell-substrate adhesions, and the magnitude of the adhesion stress can influence cell behavior, including cell spreading, migration, or signaling processes.

Shear Stress. In certain experiments, the cantilever probe may exert shear forces on the cell surface. Shear stress (occurs when parallel forces act in opposite directions along the cell surface) can cause the cell membrane to deform or experience frictional forces. Such stresses can affect cell adhesion, membrane integrity, and signaling pathways.

Tensile Stress. Tensile stress occurs when the AFM cantilever probe pulls on the cell surface, causing the cell membrane to stretch/elongate. This stress can influence cell mechanics, cytoskeletal rearrangements and the behavior of cell membrane receptors involved in adhesion and signaling.

Compression Stress. Compression stress arises when the AFM cantilever probe pushes against the cell surface, leading to cell compression or deformation. It can affect cell morphology, cytoskeletal organization, and cellular responses associated with mechanotransduction.

Notably, the applied stresses during AFM-SCFS are typically controlled and measured to ensure they remain within a biologically relevant range and not cause excessive damage to the cells. Careful consideration of the experimental parameters, such as force magnitude, loading rate, and duration of force application, is crucial to maintaining cell viability and obtaining meaningful data from AFM-SCFS experiments.

SCFS and Mechanotransduction

During AFM-SCFS, the application of nanoNewton (nN) or picoNewton (pN) forces to the cell membrane can have significant implications for mechanotransduction (the process by which cells sense and respond to mechanical stimuli, converting mechanical forces into biochemical signals) [163]. When the AFM probe applies a controlled force to the cell membrane, it can induce mechanical deformation in the membrane and the underlying cytoskeleton. This deformation can trigger a cascade of cellular responses and biochemical signaling pathways involved in mechanotransduction. The forces applied during AFM-SCFS can elicit various cellular responses. For instance, the stretching or compression of cell membrane proteins can activate mechanosensitive ion channels, leading to changes in ion flux and cellular electrical properties [164]. These ion fluxes can initiate intracellular signaling pathways that regulate cell behavior, such as cell proliferation, differentiation, migration, and gene expression.

Furthermore, the interaction forces between the AFM probe and cell membrane receptors or adhesion molecules can activate specific signaling pathways involved in mechanotransduction. These pathways can involve the recruitment of focal adhesion proteins, such as integrins, leading to the formation of focal adhesions and cytoskeletal rearrangements. These mechanical cues can influence cell adhesion, cell-cell interactions, and tissue remodeling. By precisely controlling the applied forces during AFM-SCFS, it becomes possible to study the response of cells to mechanical stimuli and investigate the mechanotransduction pathways involved.

5.8. Fate of a cell in contact with implants during SCFS

In SCFS, after the cell is brought into contact with the nano-engineered implant surface, the fate of the cells depends on the specific experimental design and the intended purpose of the study. Here are a few possible scenarios:

- **Cell Viability and Survival.** In some experiments, the goal is to investigate the adhesion properties or mechanical behavior of live cells. In such cases, efforts are made to ensure the viability and survival of the cells throughout the experiment. After the force measurement, the cells can be gently detached from the nanoscale surface and returned to a suitable growth medium for further culture or analysis.
- **Cell Damage or Detachment.** In certain cases, the applied forces or interactions with the nanoscale surface may cause cellular damage or detachment. This could result in cell death or compromised viability. In these cases, the cells may not be able to be recovered for further analysis, and the focus may be on understanding the forces involved in cell detachment or the impact of nanostructures on cell behavior.
- **Fixed Cells for Post-experiment Analysis.** For some experiments, the cells are fixed after the force measurements for subsequent analysis. Fixation involves treating the cells with chemical fixatives to preserve their structure and biological components for various downstream analyses, such as immunofluorescence staining, microscopy, or molecular analysis.

5.9. How SCFS (seconds–minutes) aid in predicting implant bioactivity?

Studying the initial stages of cell adhesion onto implants (seconds to minutes) can provide valuable insights into the potential long-term implant bioactivity and implant-tissue integration, as detailed next:

- **Cellular Response Assessment.** The initial interaction between cells and an implant surface can trigger cellular events influencing the subsequent tissue response. Researchers can evaluate key cellular behaviors (attachment, spreading and signaling pathways activation) by studying the early adhesion process. These early cellular responses can indicate how the cells will interact with the implant over time and help predict the overall tissue integration.
- **Surface Compatibility Evaluation.** The implant's material and surface characteristics influence cells' adhesion onto an implant surface. By observing the initial cell adhesion, researchers can assess the compatibility between the implant surface and the surrounding tissue. If cells fail to adhere or exhibit unfavorable responses in the early stages, it may indicate poor biocompatibility or potential for implant rejection in the long term.
- **Biofilm Formation Prediction.** The attachment of microorganisms to implant surfaces is a common cause of implant-associated infections. The early adhesion of bacteria or other microorganisms onto the implant can initiate the formation of biofilms, which are highly resistant to antibiotics and immune responses. By studying the initial microbial adhesion, researchers can gain insights into the potential for biofilm formation and the likelihood of subsequent infections.
- **Optimization of Surface Modifications.** Implant surfaces can be modified to enhance their bioactivity and promote better integration with the surrounding tissue. Studying the early stages of cell adhesion allows researchers to assess the effectiveness of various surface modifications, such as coatings, textures, or bioactive molecules. This information can guide the optimization of implant surfaces to enhance long-term implant-tissue integration and minimize complications.

While studying the initial stages of cell adhesion provides essential insights, evaluating long-term effects through *in vivo* and clinical studies is crucial. Long-term studies consider factors such as tissue remodeling, immune responses, and mechanical stability, which can influence the overall success and durability of the implant. Combining short-term cell adhesion studies with long-term evaluations provides a more comprehensive understanding of implant bioactivity and implant-tissue integration.

6. AFM-SCFS of nano-engineered implants

AFM-SCFS can be utilized to characterize the properties of mammalian cells, microorganisms, viruses, cell membranes, proteins, fibrils and nucleic acids [165,51]. Next, we present the critical investigations related to nano-engineered implants using SCFS.

6.1. Adhesion of resident tissue cells

It is noteworthy that dot-like nascent adhesions and focal complexes are formed within tens of seconds at the cell-surface site before the maturation of cell-surface interactions into focal adhesions [166]. Further, cells sense and respond to surface topography, roughness, and chemical cues of the implants [167,168]. Various implant and scaffold surface modifications have permitted mechanical stimulation of cells towards enhanced bioactivity functions [45,169]. Crucial information on implant bioactivity performance can be revealed if the adhesion of a single cell (showing in-

formation about such adhesion complexes) is quantified on nano-engineered surfaces in initial few seconds or minutes. AFM-based SCFS can interact with a single cell on a nano-engineered surface and precisely record (in nano-newtons) the force of adhesion (Fig. 5).

In an extensive review, Taubenberger et al. [147] have summarized the various implant-cell interactions that have been quantified via AFM-SCFS. For instance, to test the influence of periodically grooved nanostructures (groove/summit width: 90 nm; depth: 120 nm), bovine plasma fibronectin-modified Si wafers were contacted with L929 mouse fibroblasts, followed by SCFS via AFM [170]. Similarly, interactions between osteosarcoma Saos-2 cells with glass, titanium, titanium vanadium or cobalt-chromium surfaces [171]; and mouse melanoma cells with gel nanoparticles coated silica beads [172] have also been investigated. This review will primarily focus on nano-engineered implants and the use of AFM-SCFS towards their characterization.

Electrochemically anodized TiO₂ nanostructures (nanotubes or nanopores) fabricated on Ti-based implants are emerging as a bioactive and therapeutic modification strategy [58,173,174]. In a pioneering attempt, Bertocini et al. [175] reported SCFS measurements on titania nanotubes (TNTs) modified Ti implants to investigate the early adhesion of human mesenchymal stem cells (hMSC) via SCFS. Briefly, a single hMSC was immobilized onto fibronectin-modified tipless cantilever and then approached onto the modified surfaces for 30 s before detachment to record the signature force-distance plot. The authors compared adhesion on tissue culture polystyrene substrates (TCPS), bare flat TiO₂ and anodized nanotubular TiO₂ (TNTs were annealed to enable crystallization). Towards quantifying cellular adhesion, maximum detachment force (F_{detach}), magnitude/number of force steps for tethers and length of detachment were recorded (Fig. 6). The data confirms that the highest values for detachment forces, works of detachment and lengths of detachment were observed for TCPS, while the lowest adhesion was reported for TNTs. A significant difference in the mean detachment force was observed, following the trend: TCPS (1838±80 pN) > flat TiO₂ (360±20 pN) > TNTs (268±5 pN). Overall, TCPS surfaces had the highest works of detachment for cells, whereas TNTs had the lowest. This observation is attributed to the higher number of both tether events and individual ligand-receptor interactions for TCPS (710 tethers), as compared to flat TiO₂ (468 tethers) and TNTs (358 tethers).

It is noteworthy that serum protein aggregates can adhere to TNTs and the inter-tube gaps [176,177]. For native TiO₂, protein aggregates are sparsely distributed, whereas, for TCPS, these aggregates cover the entire surface area. Hence, the difference in the number of tethers might have originated from position-dependent protein aggregation. Compared with *in vitro* cell culture studies that show the enhanced osteogenic response of TNTs whereby longer contact times (hours to days) are investigated [178], the study by Bertocini et al. [175] involved only 30 s contact time. The presented data was influenced by the initial adsorption of serum proteins, which poses a challenge for TNTs and other nano-engineered surfaces.

Fe-Pd-based ferromagnetic shape memory alloys are emerging for biomedical applications owing to potential triggers using magnetic field and superelastic behaviour [179]. In 2018, Cakir et al. [180] utilized SCFS to investigate early fibroblast adhesion to plasma-functionalized ferromagnetic shape memory alloys (Fe-Pd). Briefly, plasma polymerized L-lysine (PLL) was used to perform biopolymer modification of Fe-Pd shape memory alloy. Fe-Pd, FePd+Lysine, glass and glass+Lysine were compared to evaluate forces/work needed to fully detach an NIH 3T3 embryonic mouse fibroblast cell at five contact times (5 s, 10 s, 20 s, 40 s, and 80 s). The results revealed enhanced cell adhesion and binding affinity on PLL-Fe-Pd.

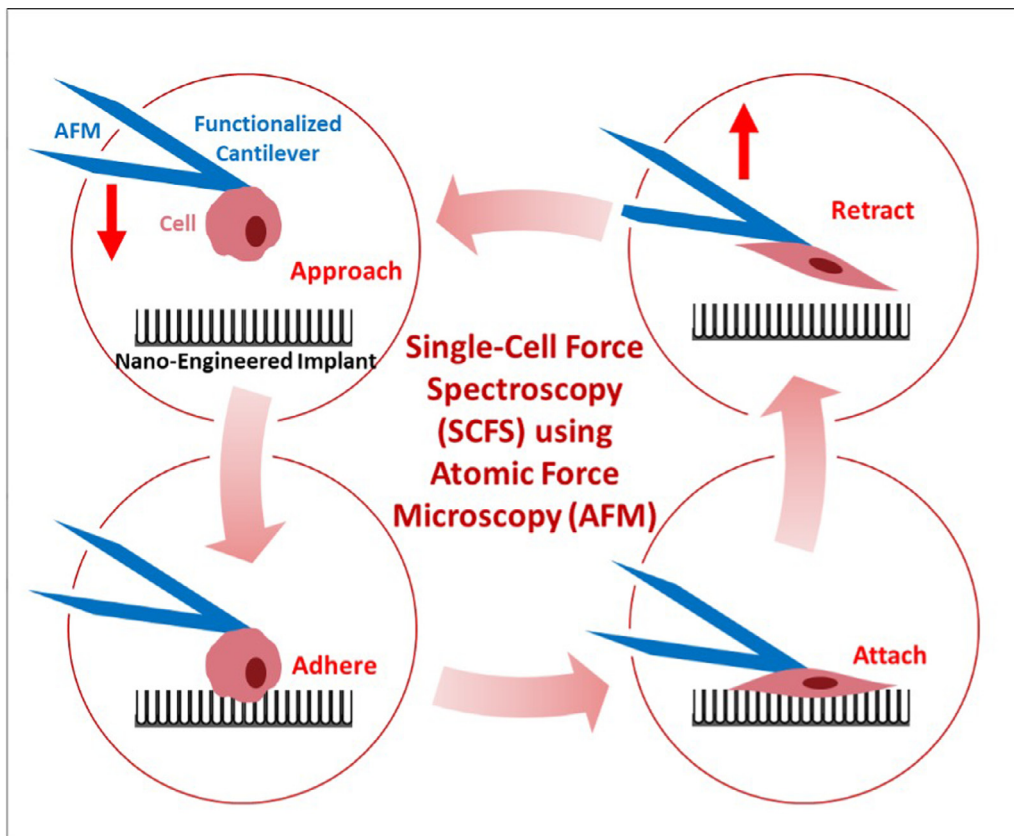


Fig. 5. Use of AFM for single-cell force spectroscopy (SCFS). Schematic representation showing *approach-adhere-attach-retract* cycle for single-cell adhesion on a nano-engineered implant surface (showing a nanoporous implant surface).

The following describes landmark investigations exploring the bioactivity of varied modified implant surfaces via AFM-SCFS:

- To provide insights into the role of RGD (Arg-Gly-Asp)-motifs in pre-osteoblast behavior, Taubenberger et al. (2010) performed SCFS using MC3T3-E1 pre-osteoblastic cells on native (Col) and partially-denatured (pdCol) collagen I substrates [181]. During the early adhesion phase (≤ 180 seconds), cellular adhesion was significantly stronger on pdCol, and exhibited a pronounced matrix mineralization activity. Further, it was revealed that pre-osteoblast adhesion to pdCol was mediated by the RGD-binding $\alpha(5)\beta(1)$ - and $\alpha(v)$ -integrins. Finally, the investigations showed that pdCol exposes RGD-motifs, which trigger the binding of $\alpha(5)\beta(1)$ - and $\alpha(v)$ -integrins that enable stimulation of osteoblast functions (adhesion, spreading and differentiation).
- To investigate how initial cell adhesion and directional migration are influenced by implant nanotopography, Lamers et al. (2012) performed AFM-SCFS using MC3T3-E1 osteoblasts on various substrates with controlled nanogrooves (itches from 150–1000nm) [182]. Initial cell adhesion was performed after 10 seconds of cell attachment, and findings revealed that initial cell adhesion was significantly induced by a 600 nm pitch and reduced by a 150 nm pitch. Next, the addition of RGD peptide significantly decreased cell adhesion, indicating that integrins/cell adhesive proteins (like fibronectin or vitronectin) are critical influencing factors in mediating specific cell adhesion on implant nanotopography.
- In 2014, Markwardt et al. fabricated a micro-rough implant using LaserCUSING® technology, followed by investigating the behavior of human osteoblasts on untreated laser-cused Ti specimens or specimens treated with different blasting agents (resulted in graded micro-roughness) [183]. Compared to blasted Ti, laser-cused Ti had the highest surface roughness, and as a result, SCFS quantification revealed the highest adhesion of osteoblasts on these surfaces.
- To advance the mechanical and bioactivity characteristics of Ti implants, Grau et al. (2017) dip-coated Selective Laser Melting (SLM)-fabricated Ti scaffolds with synthetic poly- ϵ -caprolactone (PCL) and biopolymer poly(3-hydroxybutyrate) [P(3HB)] [184]. Interestingly, no significant differences were observed between the coated Ti in osteoblast proliferation and adhesion (via SCFS).
- Using Ion Plating Plasma Assisted technology, Longo et al. (2016) coated Ti implants with thin and hard titanium carbide and nanostructured oxide layer, clustered around graphitic carbon, and investigated the bioactivity by culturing osteoblasts [185]. Briefly, the coating enhanced bone-forming ability, cellular proliferation, adhesion (confirmed via SCFS), and cell spreading.
- In 2017, Naganuma (2017) fabricated nano-rough and micro-dot/line-patterned poly-lactic acid substrates, and the SCFS analysis showed that for initial adhesion (< 1 h), nanotopography enhanced detachment force of spherical cells, while micro-topography enhanced detachment force of ‘spreading’ cells in intermediate (1–12h) and long-term (> 24 h) [186].
- Andolfi et al. (2017) utilized SCFS to interact with mouse embryonic fibroblasts with silicon nanowires (Si NWs) and observed that the cell adhesion forces with Si NWs were comparable to collagen and bare glass [187]. Further, fibroblast morphology on Si NWs exhibited high filopodia and significantly reduced mobility.
- In 2020, Herranz-Diez et al. compared biofunctionalization efficiency and cell adhesion abilities between linear RGD, cyclic

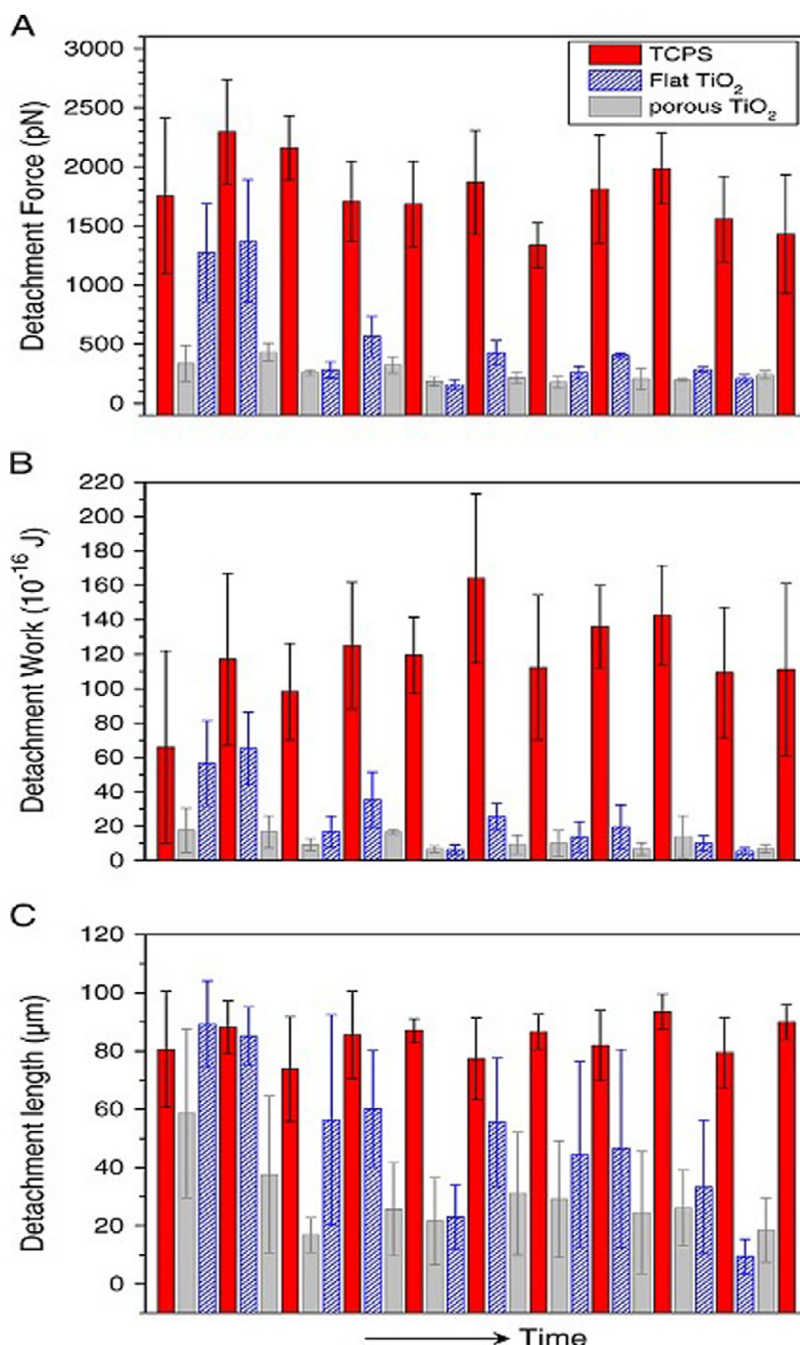


Fig. 6. Single-cell force spectroscopy for titania nanotubes (TNTs). Measurements for adhesion of a single human mesenchymal cell on TNTs: (a) detachment force; (b) work of detachment; and (c) detachment length. Adapted with permission from [175].

RGD, and recombinant fibronectin fragment III_{8–10} immobilized (physisorbed or covalently coupled) Ti and TiNbHf implants [188]. Next, using AFM-SCFS, conformation of the bioactive molecules and adhesion of rat mesenchymal stem cells on implants were investigated. Results revealed that covalent tethering provides the most optimized modification and coating with fibronectin fragment III_{8–10} augments cellular adhesion on Ti and TiNbHf.

- Targeted at orthopedic implants, Nouri-Goushki et al. (2021) utilized direct laser writing to 3D print submicron pillars [diameter 250 nm, various heights 250 - 1000 nm and interspaces] to study the interrelation between cell adhesion, cell mechanics and osteogenic potential [157]. Via AFM-SCFS, ad-

hesion force and the work of adhesion for preosteoblast cells on various substrate surfaces were studied, and the results revealed that the pillar geometry and arrangement significantly influenced adhesion parameters and focal adhesion formation.

6.2. Adhesion of Pathogenic Bacteria

Implant Fouling and Underlying Interactions

Fouling in the implant system occurs through various levels and involves a range of physical and biochemical interactions. These interactions can be categorized into unspecific and specific fouling mechanisms [189,190]:

- **Unspecific Fouling Mechanisms.** These involve non-specific interactions such as van der Waals forces, electrostatic interactions, and hydrophobic interactions. Van der Waals forces are weak attractive forces between atoms or molecules, while electrostatic interactions result from the attraction or repulsion of charged particles. Hydrophobic interactions arise between non-polar molecules in an aqueous environment. These unspecific interactions can lead to the adsorption of proteins, cells, and other biomolecules onto the implant surface, contributing to the formation of a non-specific fouling layer.
- **Specific Fouling Mechanisms.** Specific molecular recognition and binding events include the adhesion of specific proteins or cells to surface receptors or ligands on the implant. These interactions often involve biological recognition elements, such as antibodies, enzymes, or cell adhesion molecules, which mediate the binding between the implant surface and biomolecules or cells.

The combination of unspecific and specific fouling mechanisms can lead to the formation of complex fouling layers on implant surfaces [191]. The fouling layers may consist of proteins, cells, ECM components, or other biological substances. The presence of fouling layers can have detrimental effects on the function and integration of implants, such as impaired biocompatibility, compromised mechanical stability, and increased susceptibility to infection. Understanding the physical and biochemical interactions involved in implant fouling is crucial for developing strategies to minimize or prevent fouling. Surface modifications, such as anti-fouling coatings or bioactive surface functionalization, can help mitigate fouling effects and enhance the performance and longevity of implants [129,192].

Bacterial Adhesion and Mechanics

Bacterial adhesion on implants refers to the attachment and colonization of bacteria on the surface of implanted medical devices [193]. When an implant is introduced into the body, bacteria in the surrounding environment can adhere to its surface and form biofilms. Bacterial adhesion is influenced by various factors, including the surface properties of the implant, the presence of proteins or other biomolecules, and the characteristics of the surrounding tissue. Once attached, bacteria can proliferate within the biofilm, leading to the formation of a protective matrix that shields them from the host immune system and antimicrobial treatments. The mechanics of bacterial adhesion involve the interplay between the bacterial surface structures (e.g., pili or fimbriae) and the surface properties of the implant, including roughness, charge, and hydrophobicity. Understanding the mechanisms of bacterial adhesion and the associated mechanical interactions is crucial for developing strategies to prevent or mitigate implant-related infections. Bacterial adhesion on implant surfaces involves several distinct steps, each occurring at different scales of time and length [193]:

- **Adhesion** (time: seconds to minutes). Influenced by pathogen type, physiological fluids and surface characteristics, reversible adhesion of bacteria occurs on the implant surface (via Van der Waals forces and electrostatic interactions).
- **Colonization** (time: minutes to hours). Dependent on specific molecular/cellular interactions (via pili and fimbriae), bacteria accumulates and colonizes (irreversible) the implant surface that alters its surface chemistry.
- **Biofilm Formation** (time: hours to days). Formation of bacterial microcolonies and production of exopolymeric substances (EPS, consists of polysaccharides, proteins and other biomolecules) that results in biofilm formation, which protects the bacteria from pharmacological therapies.
- **Biofilm Maturation** (time: days to weeks). The entire implant surface gets covered with bacteria as a result of continuous bacterial proliferation under the protection of the biofilm that be-

comes more structurally complex and resistant to mechanical and antimicrobial treatments.

- **Persistence and Dissemination** (time: weeks to months). Mature biofilm persists on the implant surface, with bacteria continuing to multiply and disperse within the biofilm structure. Bacterial cells can detach from the biofilm and spread to other surfaces or host tissues, contributing to the risk of infection and systemic dissemination.

Notably, each step's time and length scales may vary depending on factors such as bacterial species, implant material, surface characteristics and environmental conditions. Understanding the temporal and spatial aspects of bacterial adhesion on implant surfaces is crucial for developing strategies to prevent or mitigate biofilm formation and improve the long-term success of implants.

Nano-Engineered Implants and Bacterial Adhesion

Nano-engineered implant surfaces promote cell bioactivity (functions of osteoblasts, fibroblasts or stem cells) and can augment bacterial adhesion and biofilm formation ability, attributed to nanoscale roughness and high surface area (with the exception of bioinspired bactericidal nanotopographies like nanopillars) [192,194]. Controlled nano-engineering has permitted the fabrication of various nanotopographies on implant surfaces that can provide effective bacteriostatic and bacteriocidal functions via contact killing (bed of nails mechanism) [192] or tailored elution of antibiotic agents from the surface of the nano-engineered implants [10,14].

Notably, short-time contact with bacteria is crucial to understand long-term response as the early colonizing bacteria can form a 'base layer' for secondary bacteria [195]. Studying initial bacterial adhesion can enable understanding of the underlying mechanism behind its attachment and aid in designing the next generation of bactericidal surfaces [196,197]. Using optical microscopy and cell-tracking techniques to live image bacterial cell behaviour is widely applied to investigate bacterial attachment. AFM-SCFS allows the immobilization of a single bacterial cell onto an AFM tip to evaluate mechanistic pathways, as reported elsewhere [198]. It is noteworthy that the SCFS technique allows for the simultaneous quantification of all bacterial adhesion factors *in situ* [198]. The behaviour of a single bacterium assessed via high-resolution analysis, including AFM, can direct the research in designing the next generation of responsive bactericidal surfaces. Via AFM, in physiological conditions, a single bacterium cell can be manipulated at the nanoscale, revealing crucial mechanical aspects relating to interaction with specific proteins/molecules [199].

SCFS Bacteria – Technical Aspects

It is established that proper attachment of cell to the cantilever is crucial to the SCFS procedure and for majority of microbes the bonding between the cantilever and the cell is very weak (specially for receptor-ligand based interactions) that can cause cellular detachment [200]. Hence, alternative strategies, including hydrophobic interactions [201], chemical fixation [202], glue [203], wet adhesives [204] or electrostatic interactions (poly-L-lysine [205], poly(ethyleneimine) [206]) have been developed. Beaussart et al. have described an optimized protocol for the attachment of bacteria to cantilever using bioinspired wet adhesives [200]. Briefly, the technique involves attaching a colloidal particle to the end of cantilever, followed by coating with wet adhesive polymers. Next, the viability and positioning of the attached cell are checked using a fluorescence microscope (live/dead assay).

SCFS of Bacteria on Nano-Engineered Implants

Bacterial adhesion to dental implant/material surface is a crucial step that decides biofilm formation; however, the initial contact between the implant surface and bacterial cells is poorly understood. In 2015, Hizal et al. [207] fabricated 2D nanoporous and 3D nanopillars on electropolished Ti via conventional anodization

and high stirring speed longer anodization, respectively. Next, the nano-engineered Ti surfaces were modified with layer-by-layer deposition of tannic acid (TA) and gentamicin (G). SCFS was utilized to study the adhesion of *Staphylococcus aureus* on bare and nano-engineered surfaces (without TA or G modification), and the results revealed that the adhesion force of the bacterium followed the trend: nanopillar (~2 nN) < nanoporous (~4 nN) < smooth Ti (~8 nN). Notably, bacteria with reduced adhesion are prone to be in a planktonic regime susceptible to killing via antibiotics released from the TA/G-modified implants [208]. Additionally, the bacteria adhering to the sharp nanopillars experience quick contact that can cause increased membrane stress [192].

Merghni et al. [209] investigated the adhesion of *S. aureus* adhesion on various dental restorative materials via AFM-SCFS and reported that bacterial adhesion is dependent on surface free energy and roughness, both with and without the presence of saliva. Further, Fang et al. [210] compared the adhesion of *Streptococcus sanguinis* and *Streptococcus mutans* to polyethylene terephthalate (PET) and polymethyl methacrylate (PMMA) dental materials and found that the adhesion forces of *S. mutans* to PET was significantly increased in the salivary presence. As a result, the study recommends using PMMA dental materials for patients with poor oral hygiene or high susceptibility to bacterial infection. Nanoscale adhesion of *Streptococcus sanguinis* to titanium implant surfaces has also been probed via SCFS [211]. The interaction of early colonizer *S. sanguinis* with clinically utilized smooth Ti discs revealed that adhesion force and work increased with contact times. Next, Aguayo et al. [212] used SCFS to characterize the nanoscale dynamics between *Staphylococcus aureus* and clinical implant-relevant machined Ti surfaces. With an increase in contact time from 0 s to 60 s, values of the maximum adhesion force and the total adhesion work increased. Interestingly, adding antiseptic chlorhexidine to the buffer solution increased the adhesion force and work.

In another study, Aguayo et al. [213] performed nano-indentation of *S. aureus* to planar (PL) and nanopatterned (square patterned with 120 nm pits with 300 nm centre–centre separation) SQ polycarbonate (PC) surfaces. Interestingly, similar elastic moduli were reported for bacterial interaction with PL and SQ, signifying that surface nanotopography has a minor influence on bacterial cell elasticity. Further, as expected from the nanoscale surface, SCFS confirmed that adhesion forces and work between bacteria and SQ surfaces were significantly higher at 0 s and 1 s contact times (Fig. 7). *S. aureus* adhesion forces were higher for SQ (0.10 nN at 0 s and 0.23 nN at 1 s) as compared to PL surfaces (< 0.05 nN at 0 s and 0.11 nN at 1 s). Overall, the findings suggest that contact time and surface nanotopography can dictate the early adhesion of bacteria to nano-engineered surfaces.

6.3. Quantifying sub-cellular interactions

Mechanical cues from both biological and implanted surfaces stimulate cells that sense and respond via cellular protrusions filopodia and lamellipodia [214]. Attributed to the regulation of cell biomechanics at the nanoscale (as ECM comprises nanoscale components), implant surface modification has shifted to the fabrication of controlled nanotopographies [215]. SMFS permits the use of force probes to induce single molecule unfolding and refolding, which has proven to be a versatile tool for understanding protein folding (including small single-domain to large multi-domain proteins) [216–219].

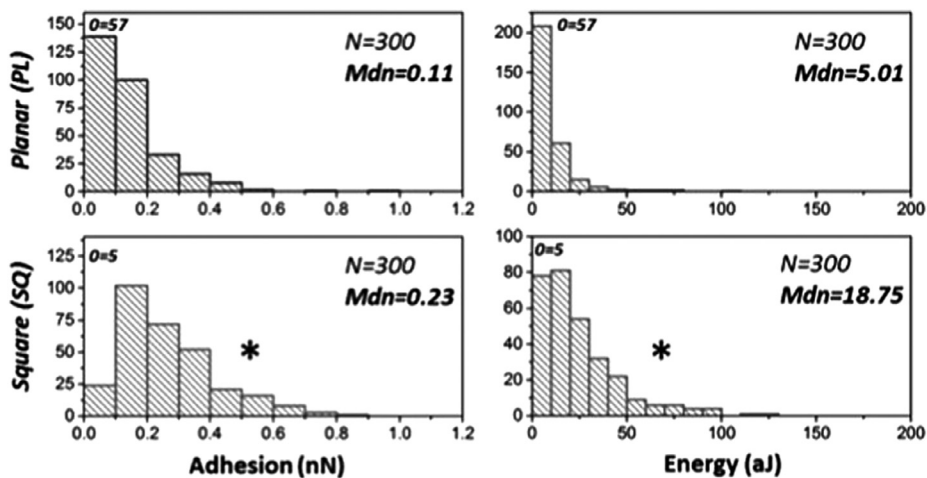
Cell membrane protrusions or filopodia play a crucial role in sensing and interacting with the environment [220], and quantification of filopodium adhesion force via SMFS onto nano-engineered implants can significantly advance the cell mechanobiology. Recently, in a pioneering attempt, Bello et al. [221] used AFM to investigate the biomechanical contribution of filopodia with

titanium nanoporous (Ti-Nano) topography obtained via oxidative chemical treatment. Briefly, filopodial lateral detachment force for MC3T3-T1 osteogenic cells cultured on polished (Ti-Control) and nanotextured Ti was studied. Via the use of contact-mode AFM, filopodia adhesion strength after 24 h of cell culture on both Ti surfaces was measured. The results (Fig. 8) revealed that nanopores exhibited strong adherence strength to filopodia, confirmed via higher resistance to lateral detachment force. Further, filopodia displacement needed significantly higher deflection of the cantilever for Ti-Nano group. The study also reported investigating variations in filopodia number and distribution and the distribution of focal adhesion on the substrates upon application of an external centrifugal force. It confirmed that implant topography dictates the adhesion characteristics of subcellular components.

7. Challenges and future directions

Recruitment of a single molecule or a single cell onto the AFM cantilever to probe the implant surface or utilize the profiling to investigate surface characteristics makes AFM a powerful tool. This is attributed to AFM's advantages, including high force resolution of minute forces (hundreds of nN) and evaluating the binding strength characterization of single-cell adhesion receptors. AFM and SMFS/SCFS can enable investigation of the influence of implant surface modification (topography, chemistry or biological) on molecular binding or cellular adhesion. However, the following challenges remain unaddressed, especially regarding SCFS that would define future work to enable the widespread and accessible utilization of AFM to its maximum potential.

- **Time/labour intensive.** Single-cell measurements and the need to record multiple force curves are both time and labour-intensive to obtain a statistically significant amount of data. Further, the analysis of the force-distance curve is time-consuming. Low-drift cantilevers are suggested to reduce thermal equilibration lag times significantly to address these challenges. Also, using multiple cantilevers [222] or cantilever-free elastomeric probe design [223] that manipulates multiple cells simultaneously is reported. Further, pressure-controlled cell capture can reduce the time for cantilever loading and calibration [224]. While the force-distance curve from SCFS provides a unique signature of the cell adhesion onto a substrate, its interpretation is not straightforward. This is attributed to the varied specific and unspecific adhesion processes that can co-occur during cell adhesion. Hence, an automatic or standardized analysis will help.
- **Studying long-term cell adhesion.** SCFS enables successful quantification of adhesion forces at very short contact times (milliseconds to minutes). At longer adhesion times, the adhesion between cell-implant can become too strong; hence, the cell cannot be detached without causing damage. Such long-term contact times may be needed for specific scenarios, for instance, observing the change in cell adhesion upon local elution of drugs/proteins from nano-engineered implants (which can take several hours) [225,226]. Additionally, cell spreading and secretion of ECM at more extended contacts can complicate effective SCFS. To enable ease of cell detachment after hours of contact, glutaraldehyde/fibronectin functionalization of cantilevers [227] or cantilevers integrated with microchannels [224] can be used. For example, Angeloni et al. used FluidFM and AFM combined with optical and electron microscopy to quantify the preosteoblast interaction on 3D printed patterns after 4 and 24 h of culture [228].
- **Protein aggregation.** Upon implantation and in contact with physiological fluids, proteins (fibronectin, vitronectin, albumin, fibrinogen, etc.) can adsorb onto the implant surface. For SCFS



* $p < 0.05$, Mann-Whitney

Fig. 7. Interacting bacteria with the nanopatterned surface. Interaction between *S. aureus* and planar (PL) or square nanopatterned (SQ) polycarbonate surfaces. Histogram showing adhesion forces and work (energy or detachment force) recorded between bacteria-functionalized cantilever and PL and SQ surfaces at a delay of 1s. Adapted with permission from [213].

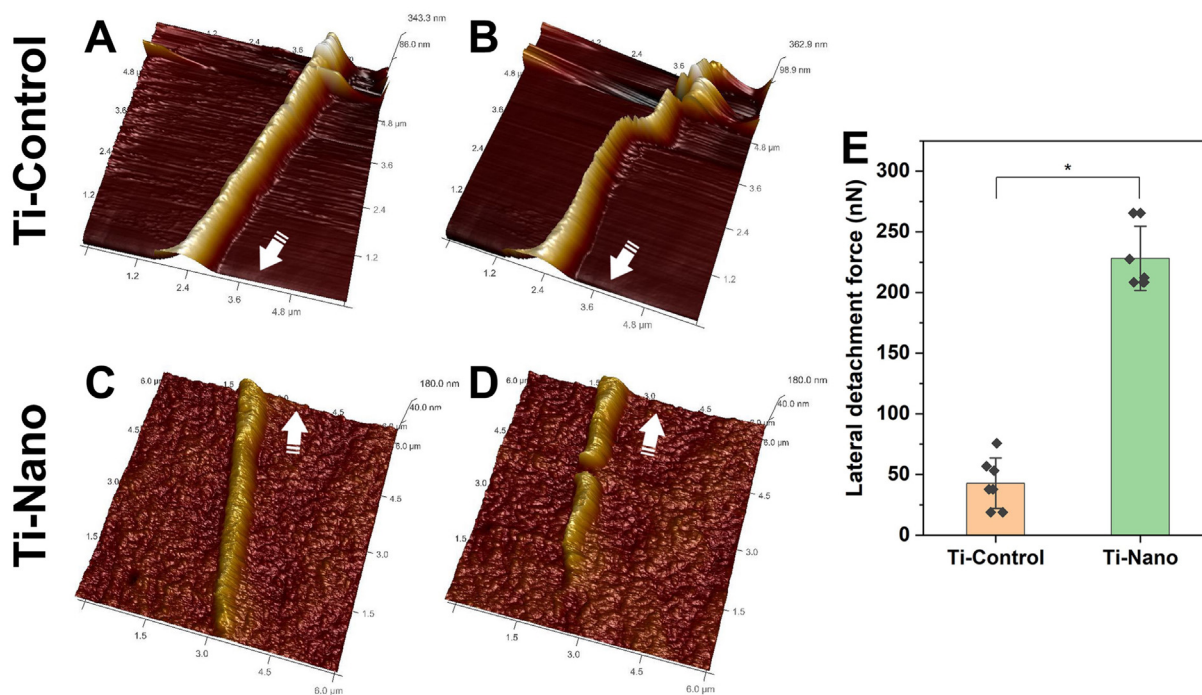


Fig. 8. Filopodia interaction with bare and nanotextured Ti. AFM images showing filopodia on Ti surfaces (A,C) before; and (B,D) after the deflection setpoint of the cantilever. Arrows represent cell body direction. (E) Lateral force analysis for detachment of filopodium from Ti surfaces. Adapted with permission from [221].

of nano-engineered implants (especially with low height variations), the amount and position of protein adsorption from serum onto nanotopographies can influence early cellular adhesion [175].

■ **Bacterial Probing and Adhesion.** Adhesion between *S. aureus* and glass substrates has shown that bacteria-substrate adhesion is proportional to the loading force applied [229]. Hence, high contact force for effective bacteria SCFS is not physiologically relevant and may augment bacteria-substrate interaction [213]. It is also noteworthy that short contact times of bacteria with nano-engineered implants demonstrate increased attachment. This information may not provide information on bacterial col-

onization and biofilm formation that requires increased contact times.

■ **Mature Cell Adhesion.** One limitation of using AFM for mature cell adhesion studies is the potential disruption of cell-substrate interactions during sample preparation and measurement. AFM typically requires the immobilization of cells on a substrate, which often involves chemical or physical methods. These processes can alter the natural cell adhesion properties and may lead to artifacts in the observed cell-substrate interactions. Additionally, applying external forces during AFM measurements can exert mechanical stress on the cells, potentially causing changes in their adhesion behavior or even detachment from

the substrate. These factors can limit the ability to study the native adhesion characteristics of mature cells accurately and may introduce uncertainties in the interpretation of AFM-based adhesion data. It is essential to carefully consider and control these potential disadvantages when utilizing AFM for mature cell adhesion studies.

AFM Limitations Driving Future Developments

- **Limited Resolution.** AFM is majorly a surface-sensitive technique, and access to the interior of living cells is restricted. Limited resolution hinders the observation of individual cell surface components, attributed to the very soft and dynamic nature of cellular surfaces. This limitation can be overcome by scanning ion-conductance microscopy (preventing physical contact with the surface and scanning using a nano-pipette).
- **Time Resolution.** Typical AFM-SCFS takes minutes to capture a high-resolution image, mainly attributed to the highly corrugated cellular surface, which is longer than the timescale at which biological dynamics operate. Ultrafast instruments, including scanning probe, allow for millisecond resolution that paves the way to understanding cellular dynamics [52].
- **Need for Optimizations.** Optimizations are required to standardize AFM-SCFS protocols, including cantilever functionalization, automated analyses and interpretation of data. This would enable ease of accessibility across various labs.
- **Cell Interior and Molecule Delivery.** To access the interior of living cells, AFM cantilever can be replaced with laser focus 3D trapping potential (photonic force microscope), or nanoparticles can be imaged inside the cells (scanning near-field ultrasonic holography). Additionally, replacing an AFM tip with a nanoneedle enables access through the membrane to the cytoplasm, permitting the delivery of specific molecules.

Take-home message

The domain crossing nano-engineered implants and their nanomechanical characterization via AFM is essential and timely for further advancements in implant bioactivity and therapy. A precise and high-resolution manipulation and measurement of the single-molecule/cell interaction combined with surface topography/roughness analysis provides a complete characterization platform. AFM with the necessary attachments can enable characterization at the various steps of nano-engineered implant development, from confirming the fabrication of nanostructures to single molecule/cellular adhesion. This review critically analyses the use of AFM-based tools to ‘profile and probe’ nano-engineered implants in predicting their bioactivity performance. Within the scope of AFM length/time scales, and the highlighted challenges, the maximum information relating to mechanobiology can be extracted via future developments and interdisciplinary collaborations.

8. Conclusions

Atomic force microscopy (AFM) enables the characterization of surface topography and single-cell/molecule interactions, which holds significant potential to understand and evaluate the performance of nano-engineered implants. Single-cell force spectroscopy (SCFS) enables recruiting a single cell as a probe attached to the AFM cantilever and utilizing the cell-cantilever to quantify the unique force signature between the cell and the modified implant surface. This special force signature shines a light on important cellular/molecular events that occur within the first few seconds/minutes of implant-cell contact and can aid in predicting the bioactivity performance of the implants. Precise quantification of cell-implant interactions in physiological conditions is a versatile tool to test various nano-engineered implants to make significant advances towards regenerative medicine and therapy. This exten-

sive review informs the reader of the key developments and research gaps in this AFM-based implant nano-biomechanical characterization.

Declaration of Competing Interest

The authors declare that they have no known competing financial interests or personal relationships that could have appeared to influence the work reported in this paper.

CRediT authorship contribution statement

Karan Gulati: Conceptualization, Investigation, Methodology, Formal analysis, Writing – original draft, Visualization. **Tajji Adachi:** Writing – review & editing, Project administration, Funding acquisition.

Funding

K.G. is the International Research Fellow of the [Japan Society for the Promotion of Science](#) (Postdoctoral Fellowships for Research in Japan (Standard)). Authors acknowledge financial support from Japan Society for the Promotion of Science (JSPS #22F20710).

Acknowledgement

The authors acknowledge support from the [Japan Society for the Promotion of Science](#) (JSPS).

References

- [1] J.C.M. Souza, M.B. Sordi, M. Kanazawa, S. Ravindran, B. Henriques, F.S. Silva, C. Aparicio, L.F. Cooper, Nano-scale modification of titanium implant surfaces to enhance osseointegration, *Acta Biomater.* 94 (2019) 112–131.
- [2] S. Minagar, C.C. Berndt, J. Wang, E. Ivanova, C. Wen, A review of the application of anodization for the fabrication of nanotubes on metal implant surfaces, *Acta Biomater.* 8 (8) (2012) 2875–2888.
- [3] K. Harawaza, B. Cousins, P. Roach, A. Fernandez, Modification of the surface nanotopography of implant devices: a translational perspective, *Mater Today Bio* 12 (2021) 100152.
- [4] D. Chopra, A. Jayasree, T. Guo, K. Gulati, S. Ivanovski, Advancing dental implants: Bioactive and therapeutic modifications of zirconia, *Bioact. Mater.* 13 (2022) 161–178.
- [5] Y. Zeng, J. Hoque, S. Varghese, Biomaterial-assisted local and systemic delivery of bioactive agents for bone repair, *Acta Biomater.* 93 (2019) 152–168.
- [6] D. Salthouse, K. Novakovic, C.M.U. Hilken, A.M. Ferreira, Interplay between biomaterials and the immune system: challenges and opportunities in regenerative medicine, *Acta Biomater.* (2022).
- [7] L. Bacakova, E. Filova, M. Parizek, T. Ruml, V. Svorcik, Modulation of cell adhesion, proliferation and differentiation on materials designed for body implants, *Biotechnol. Adv.* 29 (6) (2011) 739–767.
- [8] N.D. Gallant, K.E. Michael, A.J. Garcia, Cell adhesion strengthening: contributions of adhesive area, integrin binding, and focal adhesion assembly, *Mol. Biol. Cell* 16 (9) (2005) 4329–4340.
- [9] N. Nakao, K. Maki, M.R.K. Mofrad, T. Adachi, Talin is required to increase stiffness of focal molecular complex in its early formation process, *Biochem. Biophys. Res. Commun.* 518 (3) (2019) 579–583.
- [10] K. Gulati, D. Chopra, N. Asli Kocak-Oztug, E. Verron, Fit and forget: the future of dental implant therapy via nanotechnology, *Adv. Drug. Deliv. Rev.* (2023) 114900.
- [11] K. Gulati, Surface Modification of Titanium Dental Implants, Springer Nature, 2023.
- [12] T. Guo, K. Gulati, H. Arora, P. Han, B. Fournier, S. Ivanovski, Race to invade: understanding soft tissue integration at the transmucosal region of titanium dental implants, *Dent. Mater.* 37 (5) (2021) 816–831.
- [13] T. Albrektsson, A. Wennerberg, On osseointegration in relation to implant surfaces, *Clin. Implant Dent. Relat. Res.* 21 (2019) 4–7.
- [14] K. Gulati, C. Ding, T. Guo, H. Guo, H. Yu, Y. Liu, Craniofacial therapy: advanced local therapies from nano-engineered titanium implants to treat craniofacial conditions, *Int. J. Oral Sci.* 15 (1) (2023) 15.
- [15] Y. Zhou, J. Du, Atomic force microscopy (AFM) and its applications to bone-related research, *Prog. Biophys. Mol. Biol.* 176 (2022) 52–66.
- [16] S. Fang, Y.H. Hu, Open the door to the atomic world by single-molecule atomic force microscopy, *Matter* 4 (4) (2021) 1189–1223.
- [17] J. Friedrichs, K.R. Legate, R. Schubert, M. Bharadwaj, C. Werner, D.J. Müller, M. Benoit, A practical guide to quantify cell adhesion using single-cell force spectroscopy, *Methods* 60 (2) (2013) 169–178.

- [18] K.A. Beningo, C.M. Lo, Y.L. Wang, Flexible polyacrylamide substrata for the analysis of mechanical interactions at cell-substratum adhesions, *Methods Cell Biol.* 69 (2002) 325–339.
- [19] R. Ungai-Salánki, B. Peter, T. Gerecsei, N. Orgovan, R. Horvath, B. Szabó, A practical review on the measurement tools for cellular adhesion force, *Adv. Colloid Interface Sci.* 269 (2019) 309–333.
- [20] P.-H. Puech, K. Poole, D. Knebel, D.J. Müller, A new technical approach to quantify cell–cell adhesion forces by AFM, *Ultramicroscopy* 106 (8) (2006) 637–644.
- [21] J. Helenius, C.-P. Heisenberg, H.E. Gaub, D.J. Müller, Single-cell force spectroscopy, *J. Cell Sci.* 121 (11) (2008) 1785–1791.
- [22] H. Miyoshi, J. Ju, S.M. Lee, D.J. Cho, J.S. Ko, Y. Yamagata, T. Adachi, Control of highly migratory cells by microstructured surface based on transient change in cell behavior, *Biomaterials* 31 (33) (2010) 8539–8545.
- [23] Y. Xu, R. Zhao, Chapter 2 - Force-sensing micropillar arrays for cell mechanics and mechanobiology, in: X. Liu, Y. Sun (Eds.), *Micro and Nano Systems for Biophysical Studies of Cells and Small Organisms*, Academic Press, 2021, pp. 23–42.
- [24] K. Maki, S.-W. Han, T. Adachi, β -Catenin as a tension transmitter revealed by AFM nanomechanical testing, *Cell. Mol. Bioeng.* 8 (1) (2015) 14–21.
- [25] D.J. Müller, Y.F. Dufreñe, Atomic force microscopy as a multifunctional molecular toolbox in nanobiotechnology, *Nat. Nanotechnol.* 3 (5) (2008) 261–269.
- [26] G. Kada, F. Kienberger, P. Hinterdorfer, Atomic force microscopy in bionanotechnology, *Nano Today* 3 (1–2) (2008) 12–19.
- [27] M. Li, Chapter 1 - Fundamentals and methods of atomic force microscopy for biophysics, in: M. Li (Ed.), *Atomic Force Microscopy for Nanoscale Biophysics*, Academic Press, 2023, pp. 1–42.
- [28] S. Gowri, T. Umasankareswari, R. Joseph Rathish, S. Santhana Prabha, S. Rajendran, A. Al-Hashem, G. Singh, C. Verma, Chapter 8 - Atomic force microscopy technique for corrosion measurement, in: J. Aslam, C. Verma, C. Mustansar Hussain (Eds.), *Electrochemical and Analytical Techniques for Sustainable Corrosion Monitoring*, Elsevier, 2023, pp. 121–140.
- [29] A. Meister, M. Gabi, P. Behr, P. Studer, J. Vörös, P. Niedermann, J. Bitterli, J. Polesel-Maris, M. Liley, H. Heinzelmann, T. Zambelli, FluidFM: combining atomic force microscopy and nanofluidics in a universal liquid delivery system for single cell applications and beyond, *Nano Lett.* 9 (6) (2009) 2501–2507.
- [30] J. Xiao, Y.F. Dufreñe, Optical and force nanoscopy in microbiology, *Nat. Microbiol.* 1 (11) (2016).
- [31] O. Guillaume-Gentil, E. Potthoff, D. Ossola, C.M. Franz, T. Zambelli, J.A. Vorholt, Force-controlled manipulation of single cells: from AFM to FluidFM, *Trends Biotechnol.* 32 (7) (2014) 381–388.
- [32] M. Li, L. Liu, T. Zambelli, FluidFM for single-cell biophysics, *Nano Res.* 15 (2) (2022) 773–786.
- [33] Á.G. Nagy, N. Kanyó, A. Vörös, I. Székács, A. Bonyár, R. Horvath, Population distributions of single-cell adhesion parameters during the cell cycle from high-throughput robotic fluidic force microscopy, *Sci. Rep.* 12 (1) (2022) 7747.
- [34] M. Sztilkovic, T. Gerecsei, B. Peter, A. Saffics, S. Kurunczi, I. Szekacs, B. Szabo, R. Horvath, Single-cell adhesion force kinetics of cell populations from combined label-free optical biosensor and robotic fluidic force microscopy, *Sci. Rep.* 10 (1) (2020) 61.
- [35] F. Variola, J.B. Brunski, G. Orsini, P. Tamascio de Oliveira, R. Wazen, A. Nanci, Nanoscale surface modifications of medically relevant metals: state-of-the-art and perspectives, *Nanoscale* 3 (2) (2011) 335–353.
- [36] G. Mendonça, D.B.S. Mendonça, F.J.L. Aragão, L.F. Cooper, Advancing dental implant surface technology - From micron- to nanotopography, *Biomaterials* 29 (28) (2008) 3822–3835.
- [37] R. del Olmo, M. Czerwiński, A. Santos-Coquillat, V. Dubey, S.J. Dhoble, M. Michalska-Domańska, Nano-scale surface modification of dental implants: fabrication, in: K. Gulati (Ed.), *Surface Modification of Titanium Dental Implants*, Springer International Publishing, Cham, 2023, pp. 83–116.
- [38] K. Gulati, A. Santos, D. Findlay, D. Losic, Optimizing anodization conditions for the growth of titania nanotubes on curved surfaces, *J. Phys. Chem. C* 119 (28) (2015) 16033–16045.
- [39] J. Ballarre, T. Aydemir, L. Liverani, J.A. Roether, W. Goldmann, A.R. Boccacini, Versatile bioactive and antibacterial coating system based on silica, gentamicin, and chitosan: Improving early stage performance of titanium implants, *Surf. Coat. Technol.* 381 (2020) 125138.
- [40] A. Cerqueira, F. Romero-Gavilan, N. Araujo-Gomes, I. Garcia-Arnaez, C. Martinez-Ramos, S. Ozturan, M. Azkargorta, F. Elortza, M. Gurruchaga, J. Suay, A possible use of melatonin in the dental field: Protein adsorption and in vitro cell response on coated titanium, *Mater. Sci. Eng. C* 116 (2020) 111262.
- [41] K. von der Mark, J. Park, S. Bauer, P. Schmuki, Nanoscale engineering of biomimetic surfaces: cues from the extracellular matrix, *Cell Tissue Res.* 339 (1) (2010) 131–153.
- [42] S. Dobbenga, L.E. Fratila-Apachitei, A.A. Zadpoor, Nanopattern-induced osteogenic differentiation of stem cells - a systematic review, *Acta Biomater.* 46 (2016) 3–14.
- [43] P. Han, T. Guo, A. Jayasree, G.A. Gomez, K. Gulati, S. Ivanovski, Tunable nano-engineered anisotropic surface for enhanced mechanotransduction and soft-tissue integration, *Nano Res.* 16 (2023) 7293–7303.
- [44] J. Luo, M. Walker, Y. Xiao, H. Donnelly, M.J. Dalby, M. Salmeron-Sanchez, The influence of nanotopography on cell behaviour through interactions with the extracellular matrix - a review, *Bioact Mater* 15 (2022) 145–159.
- [45] K. Gulati, H.-J. Moon, P.T.S. Kumar, P. Han, S. Ivanovski, Anodized anisotropic titanium surfaces for enhanced guidance of gingival fibroblasts, *Mater. Sci. Eng. C* 112 (2020) 110860.
- [46] T. Guo, K. Gulati, H. Arora, P. Han, B. Fournier, S. Ivanovski, Orchestrating soft tissue integration at the transmucosal region of titanium implants, *Acta Biomater.* 124 (2021) 33–49.
- [47] A.W. Orr, B.P. Helmke, B.R. Blackman, M.A. Schwartz, Mechanisms of mechanotransduction, *Dev. Cell* 10 (1) (2006) 11–20.
- [48] M. Crisp, Q. Liu, K. Roux, J. Rattner, C. Shanahan, B. Burke, P.D. Stahl, D. Hodzic, Coupling of the nucleus and cytoplasm: role of the LINC complex, *J. Cell Biol.* 172 (1) (2006) 41–53.
- [49] M. Dalby, M. Riehle, H. Johnstone, S. Affrossman, A. Curtis, Investigating the limits of filopodial sensing: a brief report using SEM to image the interaction between 10 nm high nano-topography and fibroblast filopodia, *Cell Biol. Int.* 28 (3) (2004) 229–236.
- [50] L.E. McNamara, T. Sjöström, K. Seunarine, R.D. Meek, B. Su, M.J. Dalby, Investigation of the limits of nanoscale filopodial interactions, *J. Tissue Eng.* 5 (2014) 2041731414536177.
- [51] M. Krieg, G. Fläschner, D. Alsteens, B.M. Gaub, W.H. Roos, G.J.L. Wuite, H.E. Gaub, C. Gerber, Y.F. Dufreñe, D.J. Müller, Atomic force microscopy-based mechanobiology, *Nat. Rev. Phys.* 1 (1) (2019) 41–57.
- [52] D.J. Müller, Y.F. Dufreñe, Atomic force microscopy: a nanoscopic window on the cell surface, *Trends Cell Biol.* 21 (8) (2011) 461–469.
- [53] D.J. Müller, J. Helenius, D. Alsteens, Y.F. Dufreñe, Force probing surfaces of living cells to molecular resolution, *Nat. Chem. Biol.* 5 (6) (2009) 383–390.
- [54] D. Fotiadis, S. Scheuring, S.A. Müller, A. Engel, D.J. Müller, Imaging and manipulation of biological structures with the AFM, *Micron* 33 (4) (2002) 385–397.
- [55] T. Guo, N.A.K. Oztug, P. Han, S. Ivanovski, K. Gulati, Untwining the topography-chemistry interdependence to optimize the bioactivity of nano-engineered titanium implants, *Appl. Surf. Sci.* 570 (2021) 151083.
- [56] K. Gulati, H.-J. Moon, T. Li, P.T. Sudheesh Kumar, S. Ivanovski, Titania nanopores with dual micro-/nano-topography for selective cellular bioactivity, *Mater. Sci. Eng. C* 91 (2018) 624–630.
- [57] T. Guo, S. Ivanovski, K. Gulati, Fresh or aged: Short time anodization of titanium to understand the influence of electrolyte aging on titania nanopores, *J. Mater. Sci. Technol.* 119 (2022) 245–256.
- [58] T. Guo, N.A.K. Oztug, P. Han, S. Ivanovski, K. Gulati, Old is gold: electrolyte aging influences the topography, chemistry, and bioactivity of anodized TiO₂ nanopores, *ACS Appl. Mater. Interfaces* 13 (7) (2021) 7897–7912.
- [59] N.P. Lang, G.E. Salvi, G. Huynh-Ba, S. Ivanovski, N. Donos, D.D. Bosshardt, Early osseointegration to hydrophilic and hydrophobic implant surfaces in humans, *Clin. Oral Implants Res.* 22 (4) (2011) 349–356.
- [60] D. Chopra, T. Guo, S. Ivanovski, K. Gulati, Single-step nano-engineering of multiple micro-rough metals via anodization, *Nano Res.* 16 (1) (2023) 1320–1329.
- [61] N. Jiang, Z. Guo, D. Sun, B. Ay, Y. Li, Y. Yang, P. Tan, L. Zhang, S. Zhu, Exploring the mechanism behind improved osteointegration of phosphorylated titanium implants with hierarchically structured topography, *Colloids Surf. B* 184 (2019) 110520.
- [62] D.P. Oyarzún, O.E. Linarez Pérez, M. López Tejjelo, C. Zúñiga, E. Jeraldo, D.A. Geraldo, R. Arratia-Perez, Atomic force microscopy (AFM) and 3D confocal microscopy as alternative techniques for the morphological characterization of anodic TiO₂ nanoporous layers, *Mater. Lett.* 165 (2016) 67–70.
- [63] S. Mathai, P.S. Shaji, Bioactive conductive polymeric nanocomposite coating for titanium implants, in: *Materials Today: Proceedings*, 2023.
- [64] B. Chico, L. Martinez, F.J. Pérez, Nitrogen ion implantation on stainless steel: AFM study of surface modification, *Appl. Surf. Sci.* 243 (1) (2005) 409–414.
- [65] S.B. Chinnaraj, P.G. Jayathilake, J. Dawson, Y. Ammar, J. Portoles, N. Jakubovics, J. Chen, Modelling the combined effect of surface roughness and topography on bacterial attachment, *J. Mater. Sci.* 81 (2021) 151–161.
- [66] A. Mühl, P. Szabó, O. Krafcsik, Z. Aigner, J. Kopniczky, N. Ákos, G. Marada, K. Turzó, Comparison of surface aspects of turned and anodized titanium dental implant, or abutment material for an optimal soft tissue integration, *Heliyon* 8 (8) (2022) e10263.
- [67] X. Yang, C. Ma, X. Wang, C. Zhou, Inner-padded atomic force microscopy cantilever for rapid mechanical mapping, *Sens. Actuators A* 359 (2023) 114488.
- [68] R. Garcia, Nanomechanical mapping of soft materials with the atomic force microscope: methods, theory and applications, *Chem. Soc. Rev.* 49 (16) (2020) 5850–5884.
- [69] S. Sundararajan, B. Bhushan, Development of AFM-based techniques to measure mechanical properties of nanoscale structures, *Sens. Actuators A* 101 (3) (2002) 338–351.
- [70] Y.-J. Kim, K. Son, I.-C. Choi, I.-S. Choi, W.I. Park, J.-i. Jang, Exploring nanomechanical behavior of silicon nanowires: AFM bending versus nanoindentation, *Adv. Funct. Mater.* 21 (2) (2011) 279–286.
- [71] M. Maksud, M. Barua, M.R.A. Shikder, B.W. Byles, E. Pomerantseva, A. Subramanian, Tunable nanomechanical performance regimes in ceramic nanowires, *Nanotechnology* 30 (47) (2019) 47LT02.
- [72] M. Antsov, B. Polyakov, V. Zadin, M. Mets, S. Oras, M. Vahtrus, R. Löhmus, L. Dorogin, S. Vlassov, Mechanical characterisation of pentagonal gold nanowires in three different test configurations: a comparative study, *Micron* 124 (2019) 102686.
- [73] A. Morel, S. Domaschke, V. Urundolil Kumaran, D. Alexeev, A. Sadeghpour, S.N. Ramakrishna, S.J. Ferguson, R.M. Rossi, E. Mazza, A.E. Ehret, G. Fortunato,

- Correlating diameter, mechanical and structural properties of poly(l-lactide) fibres from needleless electrospinning, *Acta Biomater.* 81 (2018) 169–183.
- [74] L. Angeloni, M. Ganjian, M. Nouri-Goushki, M.J. Mirzaali, C.W. Hagen, A.A. Zadpoor, L.E. Fratila-Apachitei, M.K. Ghatkesar, Mechanical characterization of nanopillars by atomic force microscopy, *Addit. Manuf.* 39 (2021) 101858.
- [75] J. Wood, A. Hayles, R. Bright, D. Palms, K. Vasilev, J. Hasan, Nanomechanical tribological characterisation of nanostructured titanium alloy surfaces using AFM: a friction vs velocity study, *Colloids Surf. B* 217 (2022) 112600.
- [76] R. McKendry, M.E. Theoclitou, T. Rayment, C. Abell, Chiral discrimination by chemical force microscopy, *Nature* 391 (6667) (1998) 566–568.
- [77] M. Mahapatro, C. Gibson, C. Abell, T. Rayment, Chiral discrimination of basic and hydrophobic molecules by chemical force spectroscopy, *Ultramicroscopy* 97 (1) (2003) 297–301.
- [78] C.D. Frisbie, L.F. Rozsnyai, A. Noy, M.S. Wrighton, C.M. Lieber, Functional group imaging by chemical force microscopy, *Science* 265 (5181) (1994) 2071–2074.
- [79] M. Ludwig, W. Dettmann, H.E. Gaub, Atomic force microscope imaging contrast based on molecular recognition, *Biophys. J.* 72 (1) (1997) 445–448.
- [80] T. Bolland, B.D. Ratner, Direct measurement of hydrogen bonding in DNA nucleotide bases by atomic force microscopy, *Proc. Nat. Acad. Sci. U.S.A.* 92 (12) (1995) 5297–5301.
- [81] C. Xing, L. Liu, Y. Cui, D. Ding, Analysis of base bitumen chemical composition and aging behaviors via atomic force microscopy-based infrared spectroscopy, *Fuel* 264 (2020) 116845.
- [82] Z. Liu, T. Rios-Carvajal, M. Ceccato, T. Hassenkam, Nanoscale chemical mapping of oxygen functional groups on graphene oxide using atomic force microscopy-coupled infrared spectroscopy, *J. Colloid Interface Sci.* 556 (2019) 458–465.
- [83] M.A. Rickard, G.F. Meyers, B.M. Habersberger, C.W. Reinhardt, J.J. Stanley, Nanoscale chemical imaging of a deuterium-labeled polyolefin copolymer in a polyolefin blend by atomic force microscopy-infrared spectroscopy, *Polymer* 129 (2017) 247–251.
- [84] J. Yang, J. Hatcherian, P.C. Hackley, A.E. Pomerantz, Nanoscale geochemical and geomechanical characterization of organic matter in shale, *Nat. Commun.* 8 (1) (2017) 2179.
- [85] A. Dazzi, C.B. Prater, AFM-IR: Technology and applications in nanoscale infrared spectroscopy and chemical imaging, *Chem. Rev.* 117 (7) (2017) 5146–5173.
- [86] A. Liscio, V. Palermo, P. Samorì, Nanoscale quantitative measurement of the potential of charged nanostructures by electrostatic and Kelvin probe force microscopy: unraveling electronic processes in complex materials, *Acc. Chem. Res.* 43 (4) (2010) 541–550.
- [87] N.S. Malvankar, D.R. Lovley, Microbial nanowires for bioenergy applications, *Curr. Opin. Biotechnol.* 27 (2014) 88–95.
- [88] L.-Z. Cheong, W. Zhao, S. Song, C. Shen, Lab on a tip: applications of functional atomic force microscopy for the study of electrical properties in biology, *Acta Biomater.* 99 (2019) 33–52.
- [89] M. Nonnenmacher, M.P. O'Boyle, H.K. Wickramasinghe, Kelvin probe force microscopy, *Appl. Phys. Lett.* 58 (25) (1991) 2921–2923.
- [90] W. Melitz, J. Shen, A.C. Kummel, S. Lee, Kelvin probe force microscopy and its application, *Surf. Sci. Rep.* 66 (1) (2011) 1–27.
- [91] T. Hallam, C.M. Duffy, T. Minakata, M. Ando, H. Sirringhaus, A scanning Kelvin probe study of charge trapping in zone-cast pentacene thin film transistors, *Nanotechnology* 20 (2) (2009).
- [92] N.G. Clack, K. Salaita, J.T. Groves, Electrostatic readout of DNA microarrays with charged microspheres, *Nat. Biotechnol.* 26 (7) (2008) 825–830.
- [93] E. Finot, Y. Leonenko, B. Moores, L. Eng, M. Amrein, Z. Leonenko, Effect of cholesterol on electrostatics in lipid–protein films of a pulmonary surfactant, *Langmuir* 26 (3) (2010) 1929–1935.
- [94] C. Tang, J. Iwahara, G.M. Clore, Visualization of transient encounter complexes in protein–protein association, *Nature* 444 (7117) (2006) 383–386.
- [95] C. Leung, D. Maradan, A. Kramer, S. Howorka, P. Mesquida, B.W. Hoogenboom, Improved Kelvin probe force microscopy for imaging individual DNA molecules on insulating surfaces, *Appl. Phys. Lett.* 97 (20) (2010) 203703.
- [96] H. Lee, W. Lee, J.H. Lee, D.S. Yoon, Surface potential analysis of nanoscale biomaterials and devices using kelvin probe force microscopy, *J. Nanomater.* (2016).
- [97] M. Murrell, M. Welland, S. O'Shea, T. Wong, J. Barnes, A. McKinnon, M. Heyns, S. Verhaverbeke, Spatially resolved electrical measurements of SiO₂ gate oxides using atomic force microscopy, *Appl. Phys. Lett.* 62 (7) (1993) 786–788.
- [98] C. Musumeci, A. Liscio, V. Palermo, P. Samorì, Electronic characterization of supramolecular materials at the nanoscale by Conductive Atomic Force and Kelvin Probe Force Microscopies, *Mater. Today* 17 (10) (2014) 504–517.
- [99] T.S. Gehan, M. Bag, L.A. Renna, X. Shen, D.D. Algaier, P.M. Lahti, T.P. Russell, D. Venkataraman, Multiscale active layer morphologies for organic photovoltaics through self-assembly of nanospheres, *Nano Lett.* 14 (9) (2014) 5238–5243.
- [100] O.J. Dautel, M. Robitzer, J.C. Flores, D. Tondelier, F. Serein-Spirau, J.P. Lère-Porte, D. Guérin, S. Lenfant, M. Tillard, D. Vuillaume, Electroactive nanorods and nanorings designed by supramolecular association of π -conjugated oligomers, *Chemistry* 14 (14) (2008) 4201–4213.
- [101] T. Heim, T. Melin, D. Deresmes, D. Vuillaume, Localization and delocalization of charges injected in DNA, *Appl. Phys. Lett.* 85 (13) (2004) 2637–2639.
- [102] N.S. Malvankar, S.E. Yalcin, M.T. Tuominen, D.R. Lovley, Visualization of charge propagation along individual pili proteins using ambient electrostatic force microscopy, *Nat. Nanotechnol.* 9 (12) (2014) 1012–1017.
- [103] D.A. Bonnell, S.V. Kalinin, A. Kholkin, A. Gruverman, Piezoresponse force microscopy: a window into electromechanical behavior at the nanoscale, *MRS Bull.* 34 (9) (2009) 648–657.
- [104] S.V. Kalinin, E. Karapetian, M. Kachanov, Nanoelectromechanics of piezoresponse force microscopy, *Phys. Rev. B* 70 (18) (2004) 184101.
- [105] K. Ryan, J. Beirne, G. Redmond, J.I. Kilpatrick, J. Guyonnet, N.-V. Buchete, A.L. Kholkin, B.J. Rodriguez, Nanoscale piezoelectric properties of self-assembled fmoc-FF peptide fibrous networks, *ACS Appl. Mater. Interfaces* 7 (23) (2015) 12702–12707.
- [106] M. Minary-Jolandan, M.-F. Yu, Uncovering nanoscale electromechanical heterogeneity in the subfibrillar structure of collagen fibrils responsible for the piezoelectricity of bone, *ACS Nano* 3 (7) (2009) 1859–1863.
- [107] M. Nikiforov, G. Thompson, V.V. Reukov, S. Jesse, S. Guo, B. Rodriguez, K. Seal, A. Vertegel, S.V. Kalinin, Double-layer mediated electromechanical response of amyloid fibrils in liquid environment, *ACS Nano* 4 (2) (2010) 689–698.
- [108] B.Y. Lee, J. Zhang, C. Zueger, W.-J. Chung, S.Y. Yoo, E. Wang, J. Meyer, R. Ramesh, S.-W. Lee, Virus-based piezoelectric energy generation, *Nat. Nanotechnol.* 7 (6) (2012) 351–356.
- [109] Y. Liu, H.-L. Cai, M. Zelisko, Y. Wang, J. Sun, F. Yan, F. Ma, P. Wang, Q.N. Chen, H. Zheng, Ferroelectric switching of elastin, *Proc. Natl. Acad. Sci.* 111 (27) (2014) E2780–E2786.
- [110] C. Halperin, S. Mutchnik, A. Agronin, M. Molotskii, P. Urenski, M. Salai, G. Rosenman, Piezoelectric effect in human bones studied in nanometer scale, *Nano Lett.* 4 (7) (2004) 1253–1256.
- [111] G. Cochran, R. Pawluk, C. Bassett, Stress generated electric potentials in the mandible and teeth, *Arch. Oral Biol.* 12 (7) (1967) 917–925.
- [112] S. Amemiya, A.J. Bard, F.-R.F. Fan, M.V. Mirkin, P.R. Unwin, Scanning electrochemical microscopy, *Annu. Rev. Anal. Chem.* 1 (2008) 95–131.
- [113] M.A. Edwards, S. Martin, A.L. Whitworth, J.V. Macpherson, P.R. Unwin, Scanning electrochemical microscopy: principles and applications to biophysical systems, *Physiol. Meas.* 27 (12) (2006) R63.
- [114] P.M. Diakowski, H.-B. Kraatz, Detection of single-nucleotide mismatches using scanning electrochemical microscopy, *Chem. Commun.* 10 (2009) 1189–1191.
- [115] C. Zhao, G. Wittstock, Scanning electrochemical microscopy for detection of biosensor and biochip surfaces with immobilized pyrroloquinoline quinone (PQQ)-dependent glucose dehydrogenase as enzyme label, *Biosens. Bioelectron.* 20 (7) (2005) 1277–1284.
- [116] X. Li, A.J. Bard, Scanning electrochemical microscopy of HeLa cells—Effects of ferrocene methanol and silver ion, *J. Electroanal. Chem.* 628 (1–2) (2009) 35–42.
- [117] L. Abelmann, Magnetic force microscopy, in: J.C. Lindon, G.E. Tranter, D.W. Koppenaal (Eds.), *Encyclopedia of Spectroscopy and Spectrometry* (Third Edition), Academic Press, Oxford, 2017, pp. 675–684.
- [118] H. Hopster, H.P. Oepen, *Magnetic Microscopy of Nanostructures*, Springer Science & Business Media, 2006.
- [119] A. Schwarz, R. Wiesendanger, Magnetic sensitive force microscopy, *Nano Today* 3 (1) (2008) 28–39.
- [120] L. Folks, R. Woodward, The use of MFM for investigating domain structures in modern permanent magnet materials, *J. Magn. Magn. Mater.* 190 (1–2) (1998) 28–41.
- [121] R. Hoffmann, D. Bürgler, P. van Schendel, H. Hug, S. Martin, H.-J. Güntherodt, Perpendicular magnetic domains of a thin Ag/Fe/Ag film observed by magnetic force microscopy at room temperature, *J. Magn. Magn. Mater.* 250 (2002) 32–38.
- [122] M. Roseman, P. Grütter, Magnetic imaging and dissipation force microscopy of vortices on superconducting Nb films, *Appl. Surf. Sci.* 188 (3–4) (2002) 416–420.
- [123] A.A. Tseng, Advancements and challenges in development of atomic force microscopy for nanofabrication, *Nano Today* 6 (5) (2011) 493–509.
- [124] A.A. Tseng, Three-dimensional patterning of nanostructures using atomic force microscopes, *J. Vacuum Sci. Technol. B* 29 (4) (2011).
- [125] Y. Yan, Y. Geng, Z. Hu, Recent advances in AFM tip-based nanomechanical machining, *Int. J. Mach. Tools Manuf* 99 (2015) 1–18.
- [126] A. Malshe, K. Rajurkar, K. Virwani, C. Taylor, D. Bourell, G. Levy, M. Sundaram, J. McGeough, V. Kalyanasundaram, A. Samant, Tip-based nanomanufacturing by electrical, chemical, mechanical and thermal processes, *CIRP Ann.* 59 (2) (2010) 628–651.
- [127] G. Agarwal, R.R. Naik, M.O. Stone, Immobilization of histidine-tagged proteins on nickel by electrochemical dip pen nanolithography, *J. Am. Chem. Soc.* 125 (24) (2003) 7408–7412.
- [128] K. Gulati, J.-C. Scimeca, S. Ivanovski, E. Verron, Double-edged sword: therapeutic efficacy versus toxicity evaluations of doped titanium implants, *Drug Discov. Today* 26 (11) (2021) 2734–2742.
- [129] D. Chopra, K. Gulati, S. Ivanovski, Understanding and optimizing the antibacterial functions of anodized nano-engineered titanium implants, *Acta Biomater.* 127 (2021) 80–101.
- [130] M.C. Biswas, A. Chowdhury, M.M. Hossain, M.K. Hossain, 11 - Applications, drawbacks, and future scope of nanoparticle-based polymer composites, in: S. Mavinkere Rangappa, J. Parameswaranpillai, T.G. Yashas Gowda, S. Siengchin, M.O. Seydibeyoglu (Eds.), *Nanoparticle-Based Polymer Composites*, Woodhead Publishing, 2022, pp. 243–275.
- [131] G. Pletikapić, V. Žutić, I. Vinković Vrček, V. Svetličić, Atomic force microscopy characterization of silver nanoparticles interactions with marine di-

- atom cells and extracellular polymeric substance, *J. Mol. Recognit.* 25 (5) (2012) 309–317.
- [132] J.K. Vasir, V. Labhassetwar, Quantification of the force of nanoparticle–cell membrane interactions and its influence on intracellular trafficking of nanoparticles, *Biomaterials* 29 (31) (2008) 4244–4252.
- [133] A. Rai, A. Prabhune, C.C. Perry, Antibiotic mediated synthesis of gold nanoparticles with potent antimicrobial activity and their application in antimicrobial coatings, *J. Mater. Chem.* 20 (32) (2010) 6789–6798.
- [134] R. Shukla, V. Bansal, M. Chaudhary, A. Basu, R.R. Bhonde, M. Sastry, Biocompatibility of gold nanoparticles and their endocytotic fate inside the cellular compartment: a microscopic overview, *Langmuir* 21 (23) (2005) 10644–10654.
- [135] M. Potara, E. Jakab, A. Damert, O. Popescu, V. Canpean, S. Astilean, Synergistic antibacterial activity of chitosan–silver nanocomposites on *Staphylococcus aureus*, *Nanotechnology* 22 (13) (2011) 135101.
- [136] T.M. Dobrowsky, P. Panorchan, K. Konstantopoulos, D. Wirtz, Chapter 15 Live-cell single-molecule force spectroscopy, *Methods Cell Biol.* (2008) 411–432.
- [137] M. Li, Chapter 8 - Investigating the structures and mechanics of single animal cells by atomic force microscopy, in: M. Li (Ed.), *Atomic Force Microscopy for Nanoscale Biophysics*, Academic Press, 2023, pp. 219–267.
- [138] D.J. Müller, M. Krieg, D. Alsteens, Y.F. Dufrêne, New frontiers in atomic force microscopy: analyzing interactions from single-molecules to cells, *Curr. Opin. Biotechnol.* 20 (1) (2009) 4–13.
- [139] C. Arbore, L. Perego, M. Sergides, M. Capitanio, Probing force in living cells with optical tweezers: from single-molecule mechanics to cell mechanotransduction, *Biophys. Rev.* 11 (2019) 765–782.
- [140] I. De Vlaminck, C. Dekker, Recent advances in magnetic tweezers, *Annu. Rev. Biophys.* 41 (2012) 453–472.
- [141] Y. Zhang, L.-C. Yu, Microinjection as a tool of mechanical delivery, *Curr. Opin. Biotechnol.* 19 (5) (2008) 506–510.
- [142] A. Meister, M. Gabi, P. Behr, P. Studer, J.n. Vörös, P. Niedermann, J. Bitterli, J. Polesel-Maris, M. Liley, H. Heinzlmann, FluidFM: combining atomic force microscopy and nanofluidics in a universal liquid delivery system for single cell applications and beyond, *Nano Lett.* 9 (6) (2009) 2501–2507.
- [143] Á.G. Nagy, I. Székács, A. Bonyár, R. Horvath, Cell-substratum and cell-cell adhesion forces and single-cell mechanical properties in mono- and multi-layer assemblies from robotic fluidic force microscopy, *Eur. J. Cell Biol.* 101 (4) (2022) 151273.
- [144] M. Li, Chapter 7 - Nanoscale imaging and force probing of single microbial cells by atomic force microscopy, in: M. Li (Ed.), *Atomic Force Microscopy for Nanoscale Biophysics*, Academic Press, 2023, pp. 187–217.
- [145] J.D. Simpson, A. Ray, M. Koehler, D. Mohammed, D. Alsteens, Atomic force microscopy applied to interrogate nanoscale cellular chemistry and supramolecular bond dynamics for biomedical applications, *Chem. Commun.* 58 (33) (2022) 5072–5087.
- [146] J. Friedrichs, J. Helenius, D.J. Muller, Quantifying cellular adhesion to extracellular matrix components by single-cell force spectroscopy, *Nat. Protoc.* 5 (7) (2010) 1353–1361.
- [147] A.V. Taubenberger, D.W. Hutmacher, D.J. Muller, Single-cell force spectroscopy, an emerging tool to quantify cell adhesion to biomaterials, *Tissue Eng. Part B* 20 (1) (2013) 40–55.
- [148] E.P. Wojcikiewicz, X. Zhang, A. Chen, V.T. Moy, Contributions of molecular binding events and cellular compliance to the modulation of leukocyte adhesion, *J. Cell Sci.* 116 (12) (2003) 2531–2539.
- [149] X. Zhang, A. Chen, D.D. Leon, H. Li, E. Noiri, V.T. Moy, M.S. Goligorsky, Atomic force microscopy measurement of leukocyte-endothelial interaction, *Am. J. Physiol.* 286 (1) (2004) H359–H367.
- [150] A. Taubenberger, D.A. Cisneros, J. Friedrichs, P.H. Puech, D.J. Muller, C.M. Franz, Revealing early steps of alpha2beta1 integrin-mediated adhesion to collagen type I by using single-cell force spectroscopy, *Mol. Biol. Cell* 18 (5) (2007) 1634–1644.
- [151] P.-H. Puech, A. Taubenberger, F. Ulrich, M. Krieg, D.J. Muller, C.-P. Heisenberg, Measuring cell adhesion forces of primary gastrulating cells from zebrafish using atomic force microscopy, *J. Cell Sci.* 118 (18) (2005) 4199–4206.
- [152] S. Izrailev, S. Stepaniants, M. Balsara, Y. Oono, K. Schulten, Molecular dynamics study of unbinding of the avidin-biotin complex, *Biophys. J.* 72 (4) (1997) 1568–1581.
- [153] F. Pincet, J. Husson, The solution to the streptavidin-biotin paradox: the influence of history on the strength of single molecular bonds, *Biophys. J.* 89 (6) (2005) 4374–4381.
- [154] S. Marcotti, K. Maki, G.C. Reilly, D. Lacroix, T. Adachi, Hyaluronic acid selective anchoring to the cytoskeleton: an atomic force microscopy study, *PLoS One* 13 (10) (2018) e0206056.
- [155] M. Sun, J.S. Graham, B. Hegedüs, F. Marga, Y. Zhang, G. Forgacs, M. Grandbois, Multiple membrane tethers probed by atomic force microscopy, *Biophys. J.* 89 (6) (2005) 4320–4329.
- [156] P. Elter, T. Weihe, R. Lange, J. Gimsa, U. Beck, The influence of topographic microstructures on the initial adhesion of L929 fibroblasts studied by single-cell force spectroscopy, *Eur. Biophys. J.* 40 (3) (2011) 317–327.
- [157] M. Nouri-Goushki, L. Angeloni, K. Modaresifar, M. Minneboo, P.E. Boukany, M.J. Mirzaali, M.K. Ghatkesar, L.E. Fratila-Apachitei, A.A. Zadpoor, 3D-Printed Submicron Patterns Reveal the Interrelation between Cell Adhesion, Cell Mechanics, and Osteogenesis, *ACS Appl. Mater. Interfaces* 13 (29) (2021) 33767–33781.
- [158] J. Friedrichs, A. Manninen, D.J. Muller, J. Helenius, Galectin-3 regulates integrin $\alpha_2\beta_1$ -mediated adhesion to collagen-I and -IV *, *J. Biol. Chem.* 283 (47) (2008) 32264–32272.
- [159] A. Taubenberger, D.A. Cisneros, J. Friedrichs, P.-H. Puech, D.J. Muller, C.M. Franz, Revealing early steps of $\alpha_2\beta_1$ integrin-mediated adhesion to collagen Type I by using single-cell force spectroscopy, *Mol. Biol. Cell* 18 (5) (2007) 1634–1644.
- [160] E. Evans, K. Ritchie, Dynamic strength of molecular adhesion bonds, *Biophys. J.* 72 (4) (1997) 1541–1555.
- [161] G.I. Bell, Models for the specific adhesion of cells to cells, *Science* 200 (4342) (1978) 618–627.
- [162] T. Andreea, A.M. Gerald, Atomic force-multi-optical imaging integrated microscope for monitoring molecular dynamics in live cells, *J. Biomed. Opt.* 10 (6) (2005) 064023.
- [163] Z. Li, H. Lee, C. Zhu, Molecular mechanisms of mechanotransduction in integrin-mediated cell-matrix adhesion, *Exp. Cell. Res.* 349 (1) (2016) 85–94.
- [164] F. Pei, J. Liu, L. Zhang, X. Pan, W. Huang, X. Cen, S. Huang, Y. Jin, Z. Zhao, The functions of mechanosensitive ion channels in tooth and bone tissues, *Cell. Signalling* 78 (2021) 109877.
- [165] S.-W. Han, T. Tamaki, H.-K. Shin, T. Adachi, Local stiffness of osteocyte using atomic force microscopy, *J. Nanosci. Nanotechnol.* 17 (8) (2017) 5755–5758.
- [166] J.T. Parsons, A.R. Horwitz, M.A. Schwartz, Cell adhesion: integrating cytoskeletal dynamics and cellular tension, *Nat. Rev. Mol. Cell Biol.* 11 (9) (2010) 633–643.
- [167] H. Miyoshi, T. Adachi, Topography design concept of a tissue engineering scaffold for controlling cell function and fate through actin cytoskeletal modulation, *Tissue Eng. Part B* 20 (6) (2014) 609–627.
- [168] S. Matsushita, Y. Inoue, M. Hojo, M. Sokabe, T. Adachi, Effect of tensile force on the mechanical behavior of actin filaments, *J. Biomech.* 44 (9) (2011) 1776–1781.
- [169] K.O. Okeoye, Y. Kibe, T. Adachi, Controlling macroscale cell alignment in self-organized cell sheets by tuning the microstructure of adhesion-limiting micro-mesh scaffolds, *Mater. Today Adv.* 12 (2021) 100194.
- [170] P. Elter, R. Lange, U. Beck, Atomic force microscopy studies of the influence of convex and concave nanostructures on the adsorption of fibronectin, *Colloids Surf. B* 89 (2012) 139–146.
- [171] M. Benoit, H.E. Gaub, Measuring cell adhesion forces with the atomic force microscope at the molecular level, *Cells Tissues Organs* 172 (3) (2002) 174–189.
- [172] C.E. McNamee, S. Armini, S. Yamamoto, K. Higashitani, Determination of the binding of non-cross-linked and cross-linked gels to living cells by atomic force microscopy, *Langmuir* 25 (12) (2009) 6977–6984.
- [173] K. Gulati, T. Li, S. Ivanovski, Consume or conserve: microroughness of titanium implants toward fabrication of dual micro-nanotopography, *ACS Biomater. Sci. Eng.* 4 (9) (2018) 3125–3131.
- [174] D. Martinez-Marquez, K. Gulati, C.P. Carty, R.A. Stewart, S. Ivanovski, Determining the relative importance of titania nanotubes characteristics on bone implant surface performance: A quality by design study with a fuzzy approach, *Mater. Sci. Eng. C* 114 (2020) 110995.
- [175] P. Bertoncini, S.Le Chevalier, S. Lavenus, P. Layrolle, G. Louarn, Early adhesion of human mesenchymal stem cells on TiO₂ surfaces studied by single-cell force spectroscopy measurements, *J. Mol. Recognit.* 25 (5) (2012) 262–269.
- [176] S. Oh, K.S. Brammer, Y.S.J. Li, D. Teng, A.J. Engler, S. Chien, S. Jin, Stem cell fate dictated solely by altered nanotube dimension, *Proc. Natl. Acad. Sci.* 106 (7) (2009) 2130–2135.
- [177] L. Zhao, L. Liu, Z. Wu, Y. Zhang, P.K. Chu, Effects of micropitted/nanotubular titania topographies on bone mesenchymal stem cell osteogenic differentiation, *Biomaterials* 33 (9) (2012) 2629–2641.
- [178] K. Gulati, M. Kogawa, S. Maher, G. Atkins, D. Findlay, D. Losic, Titania nanotubes for local drug delivery from implant surfaces, in: D. Losic, A. Santos (Eds.), *Electrochemically Engineered Nanoporous Materials: Methods, Properties and Applications*, Springer International Publishing, Cham, 2015, pp. 307–355.
- [179] M. Zink, S.G. Mayr, Ferromagnetic shape memory alloys: synthesis, characterization and biocompatibility of Fe–Pd for mechanical coupling to cells, *Mater. Sci. Technol.* 30 (13) (2014) 1579–1589.
- [180] M.V. Cakir, U. Allenstein, M. Zink, S.G. Mayr, Early adhesion of cells to ferromagnetic shape memory alloys functionalized with plasma assembled biomolecules – a single cell force spectroscopy study, *Mater. Des.* 158 (2018) 19–27.
- [181] A.V. Taubenberger, M.A. Woodruff, H. Bai, D.J. Muller, D.W. Hutmacher, The effect of unlocking RGD-motifs in collagen I on pre-osteoblast adhesion and differentiation, *Biomaterials* 31 (10) (2010) 2827–2835.
- [182] E. Lamers, J. te Riet, M. Domanski, R. Lutjge, C.G. Figdor, J.G. Gardeniers, X.F. Walboomers, J.A. Jansen, Dynamic cell adhesion and migration on nanoscale grooved substrates, *Eur. Cell Mater.* 23 (2012) 182–193 discussion 193–4.
- [183] J. Markwardt, J. Friedrichs, C. Werner, A. Davids, H. Weise, R. Lesche, A. Weber, U. Range, H. Meißner, G. Lauer, B. Reitemeier, Experimental study on the behavior of primary human osteoblasts on laser-cured pure titanium surfaces, *J. Biomed. Mater. Res. A* 102 (5) (2010) 1422–1430.
- [184] M. Grau, J. Matena, M. Teske, S. Petersen, P. Aliuos, L. Roland, N. Grabow, H. Murua Escobar, N.C. Gellrich, H. Haferkamp, I. Nolte, Vitro evaluation of PCL and P(3HB) as coating materials for selective laser melted porous titanium implants, *Materials* 10 (12) (2017).

- [185] G. Longo, C.A. Ioannidu, A. Scotto d'Abusco, F. Superti, C. Misiano, R. Zononi, L. Politi, L. Mazzola, F. Iosi, F. Mura, R. Scandurra, Improving osteoblast response in vitro by a nanostructured thin film with titanium carbide and titanium oxides clustered around graphitic carbon, *PLoS One* 11 (3) (2016) e0152566.
- [186] T. Naganuma, The relationship between cell adhesion force activation on nano/micro-topographical surfaces and temporal dependence of cell morphology, *Nanoscale* 9 (35) (2017) 13171–13186.
- [187] L. Andolfi, A. Murello, D. Cassese, J. Ban, S. Dal Zilio, M. Lazzarino, High aspect ratio silicon nanowires control fibroblast adhesion and cytoskeleton organization, *Nanotechnology* 28 (15) (2017) 155102.
- [188] C. Herranz-Diez, Q. Li, C. Lamprecht, C. Mas-Moruno, S. Neubauer, H. Kessler, J.M. Manero, J. Guillem-Martí, C. Selhuber-Unkel, Bioactive compounds immobilized on Ti and TiNbHF: AFM-based investigations of biofunctionalization efficiency and cell adhesion, *Colloids Surf. B* 136 (2015) 704–711.
- [189] C. Van Oss, Interaction forces between biological and other polar entities in water: how many different primary forces are there? *J. Dispersion Sci. Technol.* 12 (2) (1991) 201–219.
- [190] C.J. van Oss, Long-range and short-range mechanisms of hydrophobic attraction and hydrophilic repulsion in specific and aspecific interactions, *J. Mol. Recognit.* 16 (4) (2003) 177–190.
- [191] D. Campoccia, L. Montanaro, C.R. Arciola, A review of the biomaterials technologies for infection-resistant surfaces, *Biomaterials* 34 (34) (2013) 8533–8554.
- [192] D. Chopra, K. Gulati, S. Ivanovski, Bed of nails: bioinspired nano-texturing towards antibacterial and bioactivity functions, *Mater. Today Adv.* 12 (2021) 100176.
- [193] E. Zhang, X. Zhao, J. Hu, R. Wang, S. Fu, G. Qin, Antibacterial metals and alloys for potential biomedical implants, *Bioact Mater* 6 (8) (2021) 2569–2612.
- [194] K. Modaresifar, S. Azizian, M. Ganjian, L.E. Fratila-Apachitei, A.A. Zadpoor, Bactericidal effects of nanopatterns: a systematic review, *Acta Biomater.* 83 (2019) 29–36.
- [195] M. Otto, Staphylococcal infections: mechanisms of biofilm maturation and detachment as critical determinants of pathogenicity, *Annu. Rev. Med.* 64 (1) (2013) 175–188.
- [196] S. Kreve, A.C.D. Reis, Bacterial adhesion to biomaterials: what regulates this attachment? *Jpn. Dent. Sci. Rev.* 57 (2021) 85–96.
- [197] C. Wang, J. Hou, C. van der Mei Henny, J. Busscher Henk, Y. Ren, Emergent properties in streptococcus mutans biofilms are controlled through adhesion force sensing by initial colonizers, *mBio* 10 (5) (2019) e01908–e01919.
- [198] S.A. James, N. Hilal, C.J. Wright, Atomic force microscopy studies of bioprocess engineering surfaces – imaging, interactions and mechanical properties mediating bacterial adhesion, *Biotechnol. J.* 12 (7) (2017) 1600698.
- [199] G. Longo, L.M. Rio, C. Roduit, A. Trampuz, A. Bizzini, G. Dietler, S. Kasas, Force volume and stiffness tomography investigation on the dynamics of stiff material under bacterial membranes, *J. Mol. Recognit.* 25 (5) (2012) 278–284.
- [200] A. Beaussart, S. El-Kirat-Chatel, R.M.A. Sullan, D. Alsteens, P. Herman, S. Derclaye, Y.F. Dufrene, Quantifying the forces guiding microbial cell adhesion using single-cell force spectroscopy, *Nat. Protoc.* 9 (5) (2014) 1049–1055.
- [201] T.S. Bergstrom Emerson, Y. Liu, E.R. Soto, C.A. Brown, W.G. McGimpsey, T.A. Camesano, Microscale correlation between surface chemistry, texture, and the adhesive strength of *Staphylococcus epidermidis*, *Langmuir* 22 (26) (2006) 11311–11321.
- [202] A. Razatos, Y.-L. Ong, M.M. Sharma, G. Georgiou, Molecular determinants of bacterial adhesion monitored by atomic force microscopy, *Proc. Natl. Acad. Sci.* 95 (19) (1998) 11059–11064.
- [203] W.R. Bowen, R.W. Lovitt, C.J. Wright, Atomic force microscopy study of the adhesion of *Saccharomyces cerevisiae*, *J. Colloid Interface Sci.* 237 (1) (2001) 54–61.
- [204] A. Beaussart, S. El-Kirat-Chatel, P. Herman, D. Alsteens, J. Mahillon, P. Hols, Y.F. Dufrene, Single-cell force spectroscopy of probiotic bacteria, *Biophys. J.* 104 (9) (2013) 1886–1892.
- [205] E.S. Ovchinnikova, B.P. Krom, H.C. van der Mei, H.J. Busscher, Force microscopic and thermodynamic analysis of the adhesion between *Pseudomonas aeruginosa* and *Candida albicans*, *Eur. Phys. J. E* 8 (24) (2012) 6454–6461.
- [206] D.T.L. Le, Y. Guérardel, P. Loubière, M. Mercier-Bonin, E. Dague, Measuring kinetic dissociation/association constants between *Lactococcus lactis* bacteria and mucins using living cell probes, *Biophys. J.* 101 (11) (2011) 2843–2853.
- [207] F. Hizal, I. Zhuk, S. Sukhishvili, H.J. Busscher, H.C. van der Mei, C.-H. Choi, Impact of 3D hierarchical nanostructures on the antibacterial efficacy of a bacteria-triggered self-defensive antibiotic coating, *ACS Appl. Mater. Interfaces* 7 (36) (2015) 20304–20313.
- [208] A.K. Muszanska, M.R. Nejadnik, Y. Chen, E.R. van den Heuvel, H.J. Busscher, H.C. van der Mei, W. Norde, Bacterial adhesion forces with substratum surfaces and the susceptibility of biofilms to antibiotics, *Antimicrob. Agents Chemother.* 56 (9) (2012) 4961–4964.
- [209] A. Merghni, D. Kammoun, H. Hentati, S. Janel, M. Popoff, F. Lafont, M. Aouni, M. Mastouri, Quantification of *Staphylococcus aureus* adhesion forces on various dental restorative materials using atomic force microscopy, *Appl. Surf. Sci.* 379 (2016) 323–330.
- [210] J. Fang, C. Wang, Y. Li, Z. Zhao, L. Mei, Comparison of bacterial adhesion to dental materials of polyethylene terephthalate (PET) and polymethyl methacrylate (PMMA) using atomic force microscopy and scanning electron microscopy, *Scanning* 38 (6) (2016) 665–670.
- [211] S. Aguayo, N. Donos, D. Spratt, L. Bozec, Probing the nano-adhesion of *Streptococcus sanguinis* to titanium implant surfaces by atomic force microscopy, *Int. J. Nanomed.* 11 (2016) 1443.
- [212] S. Aguayo, N. Donos, D. Spratt, L. Bozec, Nano-adhesion of *Staphylococcus aureus* onto titanium implant surfaces, *J. Dent. Res.* 94 (8) (2015) 1078–1084.
- [213] S. Aguayo, A. Strange, N. Gadegaard, M.J. Dalby, L. Bozec, Influence of biomaterial nanotopography on the adhesive and elastic properties of *Staphylococcus aureus* cells, *RSC Adv.* 6 (92) (2016) 89347–89355.
- [214] X. Wang, T. Ha, Defining single molecular forces required to activate integrin and notch signaling, *Science* 340 (6135) (2013) 991–994.
- [215] Y. Zhang, K. Gulati, Z. Li, P. Di, Y. Liu, Dental implant nano-engineering: advances, limitations and future directions, *Nanomaterials* 11 (10) (2021) 2489.
- [216] R. Petrosyan, A. Narayan, M.T. Woodside, Single-molecule force spectroscopy of protein folding, *J. Mol. Biol.* 433 (20) (2021) 167207.
- [217] C. Horejs, R. Ristl, R. Tscheliessnig, U.B. Sleytr, D. Pum, Single-molecule force spectroscopy reveals the individual mechanical unfolding pathways of a surface layer protein*, *J. Biol. Chem.* 286 (31) (2011) 27416–27424.
- [218] A. Jollymore, H. Li, Measuring “unmeasurable” folding kinetics of proteins by single-molecule force spectroscopy, *J. Mol. Biol.* 402 (3) (2010) 610–617.
- [219] K. Maki, S.-W. Han, Y. Hirano, S. Yonemura, T. Hakoshima, T. Adachi, Real-time TIRF observation of vinculin recruitment to stretched α -catenin by AFM, *Sci. Rep.* 8 (1) (2018) 1575.
- [220] N. Leijnse, L.B. Oddershede, P.M. Bendix, Helical buckling of actin inside filopodia generates traction, *Proc. Natl. Acad. Sci.* 112 (1) (2015) 136–141.
- [221] D. Guadarrama Bello, P. Moraille, S. Boughari, A. Badia, A. Nanci, Adhesion response of filopodia to an AFM lateral detachment force and functional changes after centrifugation of cells grown on nanoporous titanium, *Mater Today Bio* 14 (2022) 100250.
- [222] M. Favre, J. Polesel-Maris, T. Overstolz, P. Niedermann, S. Dasen, G. Gruener, R. Ischer, P. Vettiger, M. Liley, H. Heinzelmann, A. Meister, Parallel AFM imaging and force spectroscopy using two-dimensional probe arrays for applications in cell biology, *J. Mol. Recognit.* 24 (3) (2011) 446–452.
- [223] G. Kim, E.J. Kim, H.W. Do, M.-K. Cho, S. Kim, S. Kang, D. Kim, J. Cheon, W. Shim, Binary-state scanning probe microscopy for parallel imaging, *Nat. Commun.* 13 (1) (2022) 1438.
- [224] E. Potthoff, O. Guillaume-Gentil, D. Ossola, J. Polesel-Maris, S. LeibundGut-Landmann, T. Zambelli, J.A. Vorholt, Rapid and serial quantification of adhesion forces of yeast and mammalian cells, *PLoS One* 7 (12) (2012) e52712.
- [225] A. Jayasree, S. Ivanovski, K. Gulati, ON or OFF: Triggered therapies from anodized nano-engineered titanium implants, *J. Controlled Release* 333 (2021) 521–535.
- [226] K. Gulati, G.J. Atkins, D.M. Findlay, D. Losic, Nano-engineered titanium for enhanced bone therapy, in: *Biosensing and Nanomedicine VI*, SPIE, 2013, pp. 28–33.
- [227] C. Selhuber-Unkel, T. Erdmann, M. López-García, H. Kessler, U.S. Schwarz, J.P. Spatz, Cell adhesion strength is controlled by intermolecular spacing of adhesion receptors, *Biophys. J.* 98 (4) (2010) 543–551.
- [228] L. Angeloni, B. Popa, M. Nouri-Goushki, M. Minneboo, A.A. Zadpoor, M.K. Ghatkesar, L.E. Fratila-Apachitei, Fluidic force microscopy and atomic force microscopy unveil new insights into the interactions of preosteoblasts with 3D-printed submicron patterns, *Small* 19 (2) (2023) 2204662.
- [229] Y. Chen, A.K. Harapanahalli, H.J. Busscher, W. Norde, H.C.v.d. Mei, Nanoscale cell wall deformation impacts long-range bacterial adhesion forces on surfaces, *Appl. Environ. Microbiol.* 80 (2) (2014) 637–643.